

**Aerogel rafts allowing for the comparison
of novel solvent-based biological
formulations during the primary drying
phase of lyophilisation**

A Research Project Presented by

Ashti Saeed

For the degree of MSc in Drug Delivery

School of Life and Health Sciences

Aston University

02/09/2015

Supervisor

Dr Andrew Ingham

Contents

Abstract	6
Acknowledgements	7
Abbreviations	8
1. Introduction	10
1.1. Preparation of different formulations of silica aerogels	13
1.2. Monitoring the primary drying of SA.....	14
1.2.1. Product temperature	15
1.2.2. Corillonite (V. 2.3) sensor	17
1.2.3. The microbalance	18
1.3. Using different substances with synthesised SA	18
2. Aims and objectives	20
2.1. Aims	20
2.2. Objectives	20
3. Methodology	22
3.1. Materials	22
3.2. Methods	22
3.2.1. Hypothesis	22
3.2.2. Preparation of SA by lyophilisation cycle.	22
3.2.3 Hypothesis	24
3.2.4. Preparation of SA using only an acid or a base as a catalyst in the preparation of sol-gel	24
3.2.5 Hypothesis	25
3.2.6 Preparation of SA using different volumes and drying by lyophilisation cycle	25
3.2.7 Hypothesis	28
3.2.8. Preparation of different percentages of AG for addition to SA monitored by a thermocouple sensor	28
3.2.9. Hypothesis	30
3.2.10. Preparation of SA/AG 1% and monitoring sublimation using Corillonite and microbalance sensors	30
3.2.11 Hypothesis	32
3.2.12 Preparation of different percentages of MAT to be added to SA and monitored by a thermocouple sensor.....	33
3.2.13 Preparation of different percentages of PVA to be added to SA and monitored by a thermocouple sensor.....	34

3.2.14 Preparation of EC to be added to SA and monitored by a thermocouple sensor.....	35
3.2.15 Hypothesis	36
3.2.16 Preparation of new SA and using the recycled TEB to age its structure	36
3.2.17 The procedure for collecting liquid condenser	37
3.3 Statistical analysis	37
4. Results and Discussion	38
4.1. Results.....	38
4.1.1. Production of SA using TEB and drying with a lyophilisation process ..	38
4.1.2. The effect of using only an acid or a base catalyst to prepare sol-gel for SA synthesis	38
4.1.3. Primary drying time of SA increases with increased volumes of SA	39
4.1.4. Production of SA and AG.....	41
4.1.5. Production of SA and MAT.....	47
4.1.6. Production of SA and PVA	49
4.1.7. Productions of SA/EC	51
4.1.8. The effect of preparing new SA using the recycled TEB to age its structure without affecting the primary drying end point.....	52
4.1.9 Liquid collected from the condenser	54
4.2. Discussion	55
4.2.1 Using the novel solvent TEB as a reaction solvent during SA synthesis.	55
4.2.2. Using specific components and conditions in the methodology	56
4.2.3. Explanation of the results from preparing SA using one catalyst.....	59
4.2.4. Increased volumes lead to increased primary drying times.....	59
4.2.5. The effects of adding AG to SA formulations	60
4.2.6 The effects of different substances on SA.....	64
4.2.7 The effects of recycled TEB.....	71
4.2.8 Separation of the liquid collected from the condenser	72
5. Conclusion.....	73
6. Appendix.....	75
7. References	79

List of Figures

- Figure 1:** Phase diagram of water.....
- Figure 2:** Schematic of a typical industrial freeze-drying plant.....
- Figure 3:** Water vapour flow from the substance undergoing lyophilisation.....
- Figure 4:** A typical Lyophilisation cycle.....
- Figure 5:** Product thermocouple includes the probes and USB cable that would be used as sensors to monitor the primary drying of the SA.....
- Figure 6:** Product temperature profile during primary drying phase.....
- Figure 7:** The Corillonite Sensor (Version 2.3) is used to monitor the sublimation time.....
- Figure 8:** A schematic outline of the main work of the product thermocouple sensor undergoing the lyophilisation cycle.....
- Figure 9:** A schematic description of the steps to required to dry the SA sublimation of TEB from inside the sol-gel formation.....
- Figure 10:** A schematic description of the steps required to start the drying of SA/AG 1% by sublimation of TEB from inside the sol-gel formation....
- Figure 11:** Photographs of native or pure SA.....
- Figure 12:** Photographs of the sol-gel step in the synthesis of SA using only one catalyst.....
- Figure 13:** Chart recording the thermocouple temperatures of SA.....
- Figure 14:** Photographs of SA/AG that used sublimation of TEB from inside the sol-gel formation.....
- Figure 15:** Chart recording the product thermocouple temperatures of the two SA/AG concentrations.....
- Figure 16:** Photograph of shrinkage in SA/AG 1%.....
- Figure 17:** Charts recording the comparison of product thermocouple temperatures with the probes in the centre bottom of the vials.....
- Figure 18:** Chart recording the average analogue signals transmitted by the Corillonite sensor (version 2.3).....
- Figure 19:** Chart recording the average weight loss of SA/AG 1%.....
- Figure 20:** Photographs of SA/MAT by sublimation of TEB from inside the sol-gel formation.....
- Figure 21:** Chart recording the thermocouple temperatures resulting from adding different concentrations of MAT to SA.....
- Figure 22:** Photograph of SA/PVA 5%.....
- Figure 23:** Chart recording the thermocouple temperatures produced by adding PVA 5% to SA.....
- Figure 24:** Photograph of SA/EC 5%.....
- Figure 25:** Chart recording the thermocouple temperatures produced by SA/EC 5%.....
- Figure 26:** Charts recording comparisons of the thermocouple temperatures produced by putting the probes in the centre bottom of the vials.....
- Figure 27:** Chart depicting the remaining volume (18.16 ml \pm 0.763) of the evaporated liquid.....

- Figure 28:** Schematic of the production of SA using the TEB solvent (minus the drying step).....
- Figure 29:** Schematic representation of the AG network structure composed of bundles helices.....
- Figure 30:** The chemical structure of PVA showing the hydroxyl functional group.....
- Figure 31:** The chemical structure of EC polymer.....

List of Tables

- Table 1:** The standard lyophilisation cycles for drying pure SA and SA with different formulations according to volume (2.5, 5, 8 and 10.5 ml).....
- Table 2:** Main variations between devices used to measure the end point of primary drying for 2.5 ml of SA/AG1%.....
- Table 3:** The H and D of different formulations when adding different substances to 2.5 ml of SA during synthesis, according to Figures 17, 20, 24 and 26.....

Abstract

Silica aerogels (SA) are comprised of up to 90% air. As such, they are useful for many different techniques and delivery systems. In the present study, SA were successfully synthesised using the novel solvent tetraethyl butrane (TEB) as a reaction solvent via sol-gel formation and aging followed by a freeze-drying (lyophilisation) process. Although the TEB solvent is expensive, it could still be a suitable alternative to traditional solvents for the synthesis of SA. The TEB solvent has a relatively short required gelation time that eliminates the need for the solvent exchange process, thereby allowing for a shorter synthesis time. Moreover, TEB solvent could be recycled. The lyophilisation process is one of the most common processes in pharmaceutical production; however, it is a relatively expensive technique due to the length of time it takes to complete. To reduce the cost of this process, the sublimation time should be minimised, as this is the longest of the three phases of lyophilisation. This is why it is very important to determine the end point of the sublimation phase. The second part of this study therefore involved producing SA combined with different substances. These were monitored by several sensors to determine the end point of their primary drying. Some successful formulations were synthesised when the SA was combined with agarose (AG), mannitol (MAT), polyvinyl alcohol (PVA) and ethyl cellulose (EC). SA/AG was the basic formula that monitored by thermocouple temperature, Corionite V.2.3 and the microbalance sensors. The remaining formulations hardened the structure of the SA and significantly affected the sublimation time when measured by thermocouple sensor only. These findings suggest that SA produced by those substances (AG, MAT, PVA and EC) could decrease the end point of primary drying in the lyophilisation process and producing a better shape than pure SA.

Acknowledgements

I would like to extend my gratitude to Dr Andrew Ingham for his supervision, for his assistance and for his support and valuable comments.

Many thanks for my friends and special thanks go to Christeen and Jiteen for their ongoing help and support during the lab.

My husband and daughter deserve special appreciations and thanks for their continuous support and encouragement.

Abbreviations

AG — agarose

C — Celsius

D — diameter

DSC — differential scanning calorimetry

EC — ethyl cellulose

equ. — equation

g — gram

H — height

HCl — hydrochloric acid

MAT — mannitol

mBar — millibar

mg/mL — milligram per millilitre

min. minutes

mm — millimetre

Mwt — molecular weight

n — number of sample replicates

p — probability

PC personal computer

PVA — polyvinyl alcohol

SA/AG — silica aerogels with agarose in one formulation

SA/EC — silica aerogels with ethyl cellulose in one formulation

SA/MAT — silica aerogels with mannitol in one formulation

SA/PVA — silica aerogels with polyvinyl alcohol in one formulation

SD — standard deviation

SEM — scanning electron microscopy

TEB — tetraethyl butrane

UK — United Kingdom

US — United States

V. — Version

XRD — X-ray diffraction

1. Introduction

Many drugs, especially in their parenteral dosage forms, are unstable when in a solution state. Physical and chemical instability or degradation may occur when heat-sensitive products are in a liquid state. These pharmaceutical materials should be formulated as dried powders (solid state) to overcome this instability (Sinko *et al.*, 2011). Many technologies, such as spray-drying, sterile crystallization, powder filling and freeze drying, can be used for this purpose. These technologies all produce sterile powder products with improved stability, but freeze-drying (lyophilisation) is the most common method for drying unstable products. The lyophilisation technique can be applied in different fields, including for use with food, drugs and biological materials. Lyophilisation involves three steps: freezing, primary drying (sublimation) and secondary drying (Khairnar *et al.*, 2013)

The lyophilisation process begins by freezing the drug or product until ice crystals are formed by the refrigeration device. The next part of the process involves eliminating the solvent—which is mostly water that has frozen through sublimation—by lowering the pressure and increasing the temperature to supply heat to the product to sublimate the ice to gas (vapour). In the final step, the unfrozen water is removed during the secondary drying process (Franks and Auffret, 2007). Freeze-drying process is a multistage process that keeps the formulation stable for a long time (Bosca *et al.*, 2013). Water has three physical phases: liquid, solid and gas. These three phases all occur at pressures equal to 1000 mbar. That attributed to the triple point of water. The triple point can be defined as the existence of a solid, liquid and gas in thermodynamic equilibrium at a specific pressure and temperature (6.11 mbar and 0 °C for water; Khairnar *et al.*, 2013). Figure 1 describes the physical components of the lyophilisation process. After ice crystals are formed during the freezing step, the water is briefly changed to a gaseous state when the partial vapour pressure of the water is less than the ice vapour pressure. Therefore, when the temperature and pressure are less than they are at the triple point, the water can be sublimated to gas through the primary stage.

Finally, a rapid increase in formulation temperature occurs during the secondary drying to remove the remaining water from the solid solution (Bellissent-Funel and Teixeira, 2010; Rey, 2010).

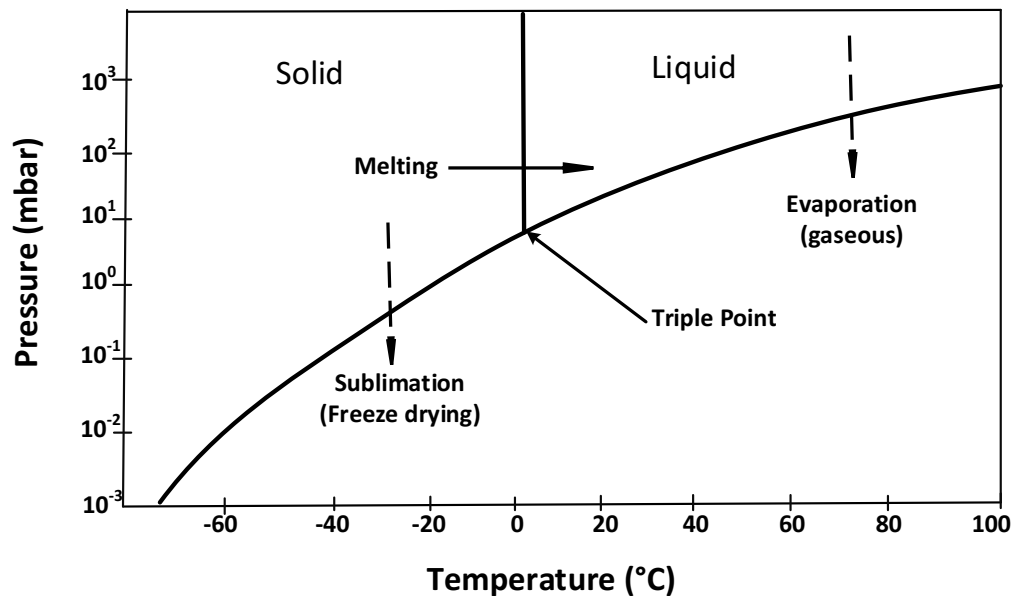


Figure 1: Phase diagram of water (adapted from Khairnar *et al.*, 2013)

Generally, the active ingredients and their excipients are prepared for freezing by being placed together in vials on the shelves. The solution is frozen through a compressor, as shown in Figure 2. The condenser is connected to the drying chamber via a duct. The drying chamber contains a valve, and after the ice has been formed, the vacuum pump evacuates the chilled condenser and the chamber. Nearly 90% of the free water should be frozen in a crystalline form while the product (e.g., the drugs) takes an amorphous shape. Remnant water (bound water) remains in the solution as an unfrozen fraction bound to the molecules in the formulation (Franks and Auffret, 2007; Akers, 2013). The freezing stage typically takes two to five hours and requires a temperature of -45 to -10 °C (Sinko *et al.*, 2011).

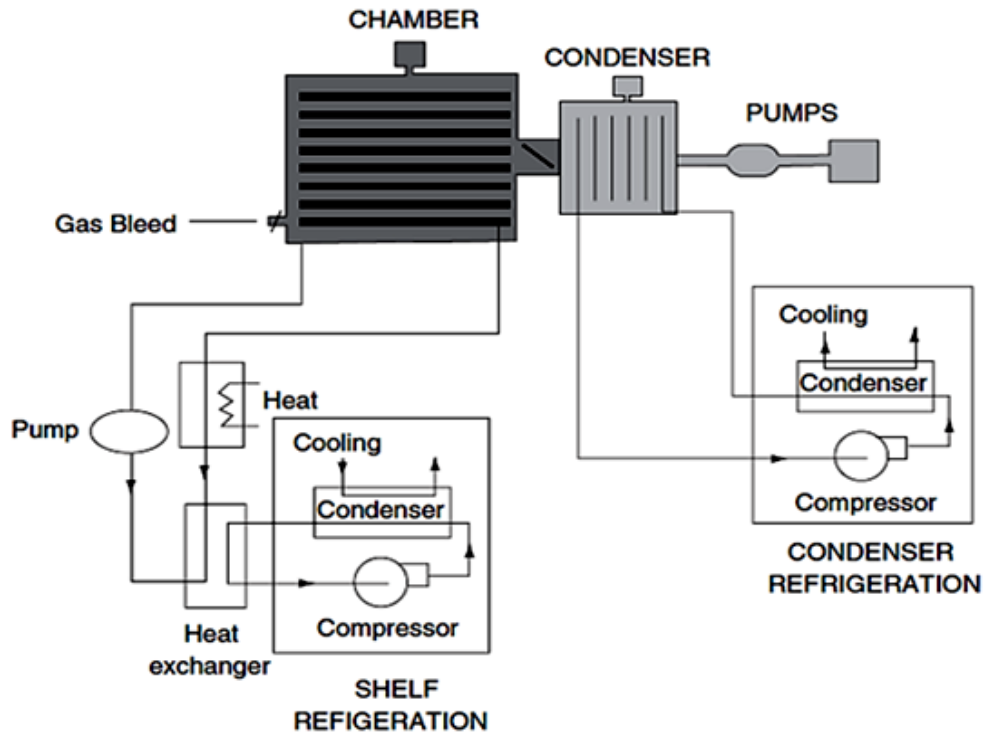


Figure 2. Schematic of a typical industrial freeze-drying plant, showing the chamber and the adjoining condenser, which can be separated by a valve; each unite is served by its own refrigeration/heating plant (Franks and Auffret ,2007).

The primary drying commences when the pressure in the drying chamber is decreased and an increase in the fluid-flowing temperature (see Figure 1). When the product is exposed to the pressure of a vacuum, a dry layer immediately forms as an outer layer of the frozen product, as shown in Figure 3. It seems that the outer layer has a porous structure, which means that the vapour flow escapes from this layer via a diffusion process. This flow of vapour through the porous layer plays an essential role in determining the rate of drying. This is considered an endothermic process, meaning that it requires heat (Mellor, 1978; Bosca *et al.*, 2013). The process typically takes place at a temperature range of -10 to -40 °C for sublimation. The duration of this process varies from five hours to five days, and the amount of residual water is usually approximately 20% (Patel and Pikal, 2009; Sinko *et al.*, 2011).

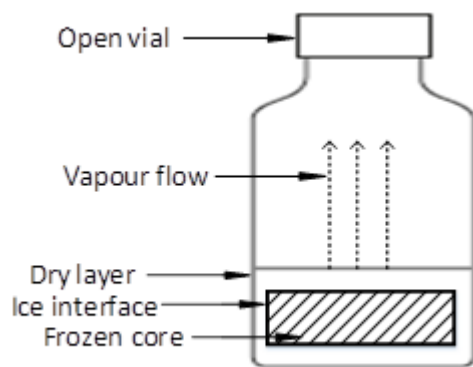


Figure 3: Water vapour flow from the substance undergoing lyophilisation (adapted from Mellor, 1987).

The secondary drying stage commences when the sublimation of the product stops. During this time, the shelf should be heated to an elevated temperature (4 °C to 50 °C, depending on the active ingredient) to eliminate the remaining water in the product using the diffusion process. Following this, desorption occurs and finally converts any unfrozen water in the condenser by evaporation (Franks and Auffret, 2007 Schneid *et al.*, 2011). This step takes anywhere from 5 to 15 hours, during which time any unfrozen water (bound water) is removed, leaving the final product to consist of only 1 to 4% of the moisture. Finally, the vials are carefully removed from the apparatus to preserve the quality of the product (Patel and Pikal, 2009; Sinko *et al.*, 2011). The next section discusses the fundamental aspects of the present research study.

1.1. Preparation of different formulations of the SA

SA are used as media for monitoring the primary drying process in this research. They have a low density (0.003 to 0.5 g /cm³), a large surface area (approximately 500 to 1,200 m²/g) with low heat conductivity (no more than 0.1 W/mk) and their structures contain up to 90% air (Brinker and Sherer, 2013). As such, they are useful for many techniques and delivery systems (Smirnova and Alrnt, 2004; Maleki *et al.*, 2013). To begin the lyophilisation cycle, the SA should be synthesised by a sol-gel procedure in the laboratory. This synthesis should take into account that SA are affected by several

factors, such as the nature of the solvent, the ratio of components and the temperature. In general, the synthesis of SA includes three main steps: preparation of the sol-gel, aging of the gel and drying of the gel (see: Methodology and Discussion) (Smirnova and Alrnt, 2004; Brinker and Sherer, 2013). Generally, to obtain the required product, the solvent should be removed from the whole gel using a different drying process, leaving the network (SiO₂) filled with air. Drying is the most important aspect of SA synthesis, and three distinct methods can be used for SA drying: supercritical drying, ambient pressure drying (evaporating drying) or a freeze-drying cycle. The present research does not address the first and second methods, as they require their own consideration and study. Although the freeze-drying process may have disadvantages—like cracks or very large and porous silica—these disadvantages can be addressed by using solvents with low expansion coefficients with rapid freezing and high sublimation pressure (Maleki *et al.*, 2013). After preparing the SA, different sensors would be used to monitoring their primary drying during lyophilisation process.

1.2. Monitoring the primary drying of SA

If the gas pressure is elevated, the rate of sublimation also rises. The vapour gas is then moved to the condenser and is usually deposited on the condenser's coils to transfer the gas to ice form (Franks and Auffret, 2007). The difference between the vapour pressure of the condenser and the vapour pressure of the ice interface is the principal force behind the sublimation process (Khairnar *et al.*, 2013). The successive primary drying method should be completed as quickly as possible, as lyophilisation is a very expensive process and this step takes the longest due to the time required to reach the target drying (Franks and Auffret, 2007). Therefore, the product temperature and the end point of the drying process usually play critical roles in determining the duration of this stage. Different tools and techniques are used to monitor these two variables.

Different tools and techniques can be used for monitoring the primary drying rate, such as pressure rise tests, thermal resistance detectors and mass spectrometers and others. In the present study, a thermocouple sensor, digital sensor and the microbalance have been used to determine the end point of the primary drying. Figure 4 shows the typical curve of the freeze-drying cycle, which can be used to determine when the primary drying and other freeze-drying process occur.

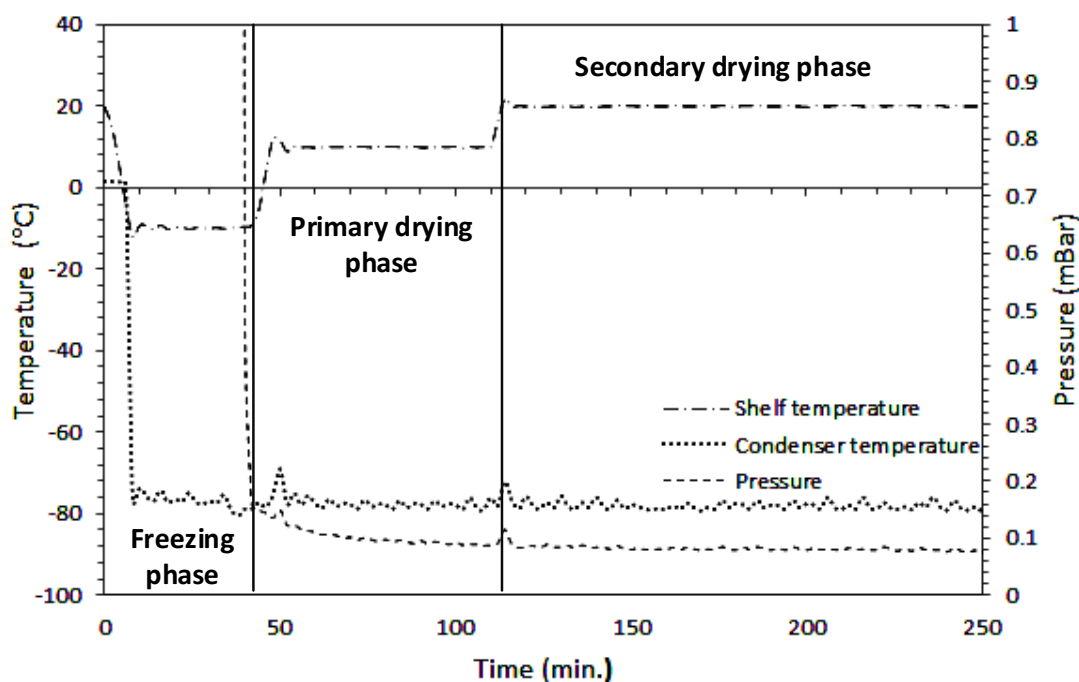


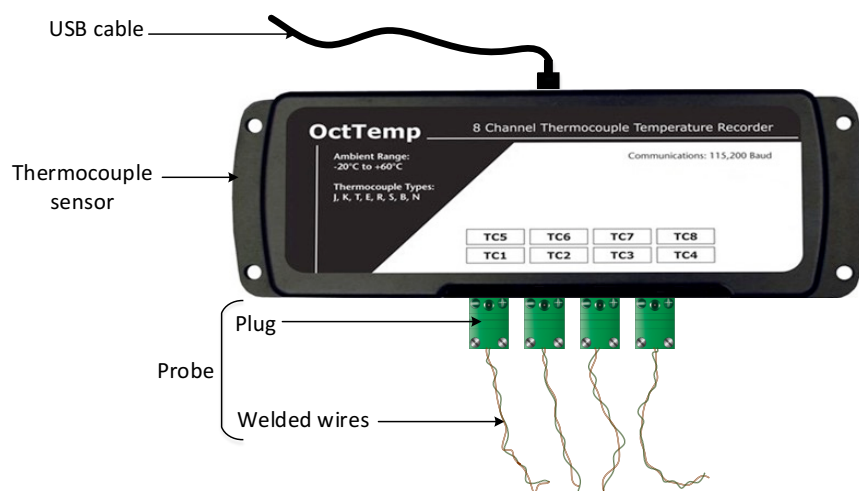
Figure 4: A typical lyophilisation cycle. Freezing occurs at -10°C for 30-40 minutes before the sample is heated to 10°C for 60 minutes. The temperature is then increased to 20°C for 6-7 h. This scheme shows an estimation of the main parts of the freeze-drying process: freezing, primary drying and secondary drying. In particular, the predicted region of the 'primary drying' was detected in this project to monitor the duration of this stage.

1.2.1. Product temperature

During lab-scale lyophilisation, the product temperature can be monitored using the thermocouple. A thermocouple is a thermo-electrical device that can be used to measure a product's temperature (Figure 5). It consists of two

different conductors (metal wires) crimped together at one spot or more (usually at their ends). Both wires should be isolated from each other. This device can produce voltage when one of the conductors produces a temperature that differs from the other conductor's temperature at the contact points (Kerlin and Johnson, 1999). For more information about the thermocouple sensor's properties, see Appendix 6.1.

Figure 6 depicts the primary drying time curve in a freeze-drying cycle; it seems that the 'offset' represents the ending point of sublimation. However, Patel *et al.* (2010) state that sublimation ends in the monitored vial(s) in the freeze-drying cycle even slightly after the onset point (as shown in Figure 6). This detail was used in the present project to determine the end point of primary drying.



Picture was adapted from:
<http://www.madgetech.com/catalogsearch/result/?q=8+channel+sensor>

Figure 5: Product thermocouple includes the probes and USB cable that would be used as sensors to monitor the primary drying of the SA.

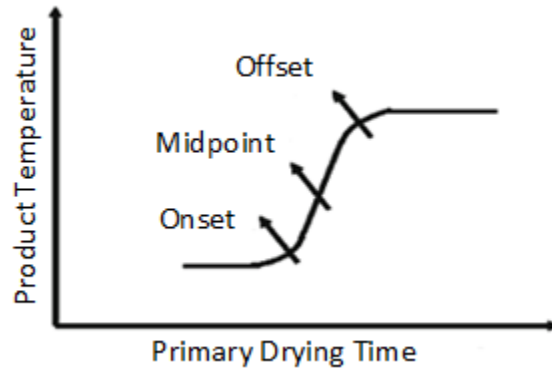


Figure 6: Product temperature profile during primary drying phase (adapted from Patel *et al.*, 2009).

1.2.2. Corillonite Sensor

It is a type of processor that converts the signal analogue to digital then allows transmitted in a standard serial protocol for display on a PC. This processor includes a circuit board with a chip connected to the sensor (light ending) that connects to the top of an SA vial (see Figure 7). It contains a microcontroller board called Arduino UNO R3 (ATmega238P), which is an open platform used for programming electronics. Arduino uses a software programme (programming the board) and a hardware program. It can read information from the sensor, which is connected to a vial as analogue signal data (10B1+ABC) during the freeze-drying cycle (Badamasi, 2014). More information about the Corillonite Sensor's properties can be found in Appendix 6.2.

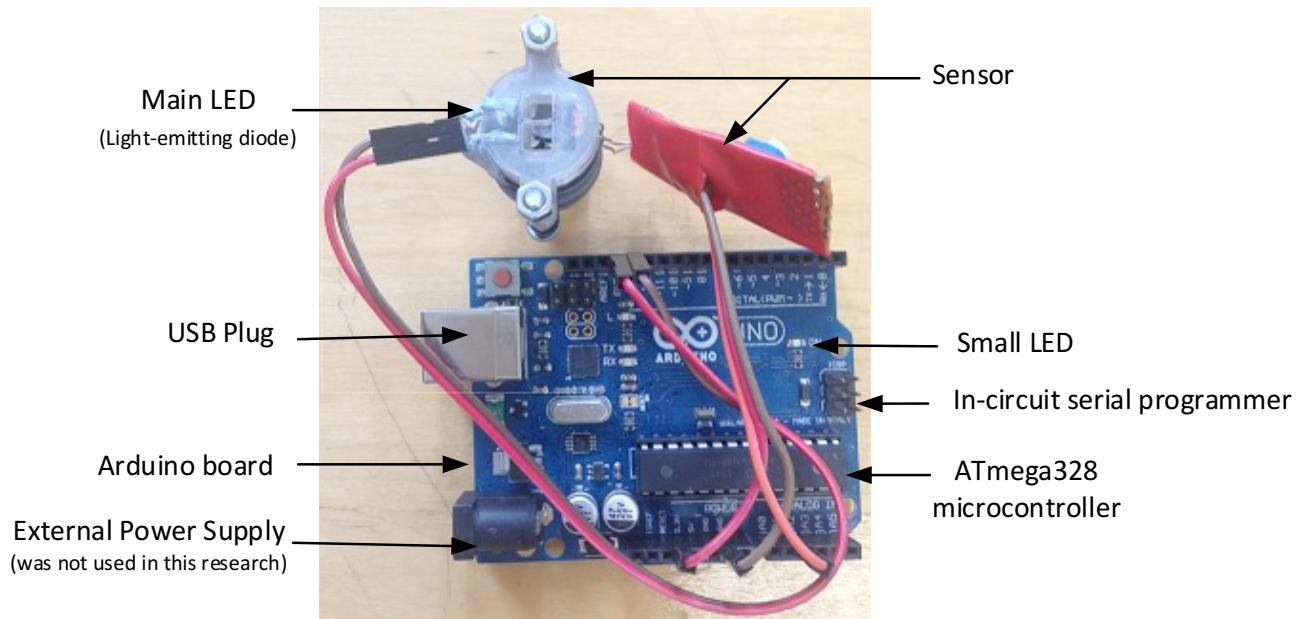


Figure 7: The Corillonite Sensor (V.2.3) is used to monitor the sublimation time. This sensor includes three main parts: the ATmega328 microcontroller board, the USB plug and the Arduino board, which programmes the software and hardware to translate the analogue (10B1+ABC).

1.2.3. The microbalance

A microbalance is a non-invasive instrument that measures the weight of a vial when it is outside of the freeze-dryer machine. Microbalances are considered one of the most useful tools for determining the end point of primary drying, although this instrument cannot measure the vials inside the chamber of a freeze-dryer. They depend on the detection of the residual moisture content (weight loss) of the SA during lyophilisation (Roth *et al.*, 2001).

1.3. Using different substances for the synthesis of SA

Substances such as AG, MAT and other different types of polymers should strengthen the SA, and they might also decrease the primary drying phase of the SA. AG substance is a linear polysaccharide that is usually extracted from the agar. It includes a trace amount of agarose sulphate and is used to

increase the strength of the media (that expect to occur when combined with the SA) (Djabourov *et al.*, 2013). MAT, which is also known as the bulking agent of lyophilisation, is one of the most common substances used with pharmaceutical products during freeze-drying to obtain the final shape. This shape depends on whether the MAT concentration is crystalline or amorphous; the latter was requested for the production of the stiff SA (Kim *et al.*, 1998).

Hydrophobic and hydrophilic polymers are assumed to increase the stiffness and compressive strength of native SA when they are added during the product's preparation. This technique is assumed to create extra strong bonds between the SA particles by increasing the connection points (Maleki *et al.*, 2013). For instance, PVA and EC—which are hydrophilic and hydrophobic polymers, respectively—can be used for this purpose. EC is cheap, a non-irritant, non-toxic and stable against light and wetness. It is classified differently according to its ethoxy contents: class T (high Mwt), class N and class K contain 49.6–51.0%, 48–49.5% and 44–47.9%, respectively (Yang, 2009; Murtaza, 2012). Also, PVA is a very tough synthetic polymer with a high tensile strength that makes it a good candidate for use as a thickener. The concentration and Mwt play important roles in obtaining the required strength and stiffing shape when the polymers are being used. PVA is graded according to its Mwt and it is either partially hydrolysed or fully hydrolysed. Fully hydrolysed PVA was used in our experiments (DeMerlis, and Schoneker, 2003; Sundararajan and Islam, 2009).

2. Aim and objectives

2.1. Aims

This research aimed to prepare the SA and different formulations of the SA with a novel solvent ('TEB') and to determine the precise endpoint of the primary drying phase by evaluating different methods that have been recommended to serve this purpose.

2.2. Objectives

Objective 1. Synthesising the SA using the TEB as a reaction solvent in the production before drying SA using the lyophilisation cycle.

Objective 2. Adding AG to the SA preparation to decrease the period of primary drying and to create a hardened, cake-shaped sample of SA to be used with all sensors and to have its primary drying time measured. This would occur as follows:

- 2.1. Using the thermocouple sensor as a control sensor to measure the product's temperature.
- 2.2. Using the Corillonite sensor to translate the analogue signals from the samples to the recorded data by using the microcontroller board to present the primary drying end point.
- 2.3. Using a microbalance to measure the decreased weight of the samples to show the end point of the sublimation.

Objective 3. Using different substances to harden the shape of the SA and to investigate the influences of these substances on the duration of the sublimation through:

- 3.1. Using different concentrations of MAT.
- 3.2. Using a hydrophilic polymer such as PVA and a hydrophobic polymer such as EC.

Objective 4. Comparing the results from various suggested substances (SA/MAT, SA/PVA and SA/EC) with pure SA according to the changes in their shapes and studying their effects on the end point of primary drying using only the thermocouple sensor for comparison.

Objective 5. Recycling the TEB solvent by:

- 5.1. Reusing the TEB solvent, otherwise known as recycled TEB, in the experiments by collecting the TEB from the aging SA (SA second step of synthesis) and using it to age the new samples of the SA.
- 5.2. Statistically comparing the effects of the recycled TEB on the primary drying time of the SA using thermocouple sensor.
- 5.3. Collecting the liquid from the condenser after it has finished its time in the freeze-dryer and trying to separate its components, including the TEB.

3. Methods and Materials

3.1. Materials

Tetramethyl orthosilicate (TMOS) 99% was obtained from Across Organics Company (Belgium), the TEB solvent was supplied by Dr Andrew Ingham (Aston University, UK) and the deionized H₂O was prepared in the laboratory. HCl 1N (standard solution), NH₄OH (25% solution in water), AG powder, MAT powder, 87–89% hydrolysed PVA and EC (ethoxy contents 48–49.5%) were supplied by Sigma-Aldrich Chemical Company (UK). The 20 ml tubing vials used for the lyophilisation cycle were purchased from Fischer Scientific (manufactured by Adelphi). The advanced hotplate stirrer was purchased from VWR International (USA), the microbalance from Kern and the Hotbox Oven with fan from Gallenkamp, UK. The freeze-dryer machine was a VirTis Wizard 2.0 (SP, USA) with one shelf (SP, USA). The Corillonite sensor (V.2.3) was supplied by Corillonite Ltd., UK, the PC was provided by HP, USA and the thermocouple sensor was an Oct Temp 8 channel supplied by Madge Tech Company (US).

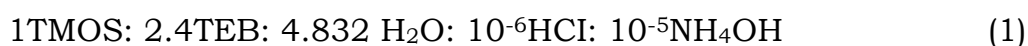
3.2. Methods

3.2.1. Hypothesis: SA will be produced from the TEB (the novel solvent) and drying (via the freeze-drying process).

3.2.2. Preparation of the SA using the lyophilisation cycle: Preparation of the SA involved three main components. These three steps were:

1. **Sol-gel formation:** This process included forming the solution (sol) and the gelation (gel). The volume of the TMOS and the volume of the H₂O were each divided into two parts (Part A and Part B) according to the molar ratio (see equ. 1, below). Part A of the TMOS was added to the TEB solvent in a beaker and stirred at 40 °C on a hot magnetic stirrer. Then, Part A of the water and HCl were added to the same beaker and

were continuously stirred until they were homogenised and hydrolysis began. This new solution was called the acid-catalyst. Part B of the TMOS was added to the acid-catalyst. After 1–2 minutes, Part B of the H₂O was added to the beaker and continuously stirred for 30 minutes at 40 °C to continue the hydrolysis. To commence the condensation step, NH₄OH was added to the acid-catalyst solution under rapid stirring for 5 minutes until the pH level was 6 at 50 °C (Pons *et al.*, 2012). The sol-gel formulation was then transferred to the vials, which were filled according to the required volume, and the vials were tightly capped with rubber stoppers and put in the oven at 65 °C for 55 minutes to form the gels. The solution was not poured when the vessel or container was tipped (Smirnova and Alrt, 2004). The end product was called sol-gel and was prepared using the following molar ratio:



- 2. Aging (or the post-gelation process):** After the gelation was formed, the vial covers were removed and new TEB was added to the vials to strengthen the structure (added 1.5-2 mL for each vial) (Brinker and Scherer, 2013). The vials were immediately capped or sealed to prevent crystallisation caused by the gels' reaction with CO₂ in the atmosphere, which would cause the samples to crack. The vials were also sealed to avoid solvent evaporation (Su *et al.*, 2012). After the vials were tightly closed, they were left for 8–20 hours at 35–40 °C to obtain the SA aging.
- 3. Drying:** The vials of SA were removed from the oven. Their covers were removed, as was the TEB solvent used in the previous step. This solvent was kept for later use (see Section 3.2.16) in a bottle labelled 'recycled TEB'. The vials were then placed in the centre of the shelf of the freeze-dryer to start the cycle of drying and 6 vials per cycle (Patel *et al.*, 2010). Table 1 shows the standard lyophilisation cycle for each volume in detail (2.5, 5, 8, 10.5 ml).

Table 1. The standard lyophilisation cycles for drying pure SA and SA with different formulations according to volume (2.5, 5, 8 and 10.5 ml).

Standard lyophilisation cycle for experiments with only 2.5 ml vials	Standard lyophilisation cycle for experiments with 5, 8 and 10.5 ml vials
<ol style="list-style-type: none"> 1. Freeze at -10 °C and hold for at least 25-30 minutes. 2. Turn on the condenser until it reaches -77 to -80 °C. 3. Turn on the vacuum to increase the pressure until it reaches 0.01–0.4 mbar. 4. Finally, set the shelf control to 10 °C for approximately 60 minutes, then heat to 20 °C for 5–6 hours. The total production time of the SA is 250 minutes. 	<ol style="list-style-type: none"> 1. Freeze at -10 °C and hold for at least 60 minutes. 2. Turn on the condenser until it reaches -77 to -80 °C. 3. Turn on the vacuum to increase the pressure until it reaches 0.02–0.5 mbar. 4. Finally, set the shelf control to 20 °C and hold for 14–16 hours. The total production time of the SA is 950 minutes.

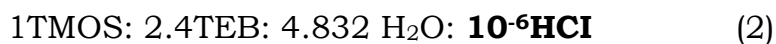
3.2.3 Hypothesis: Only acid or base can be used as a catalyst in the sol-gel step for preparing the SA (not both substances).

3.2.4. Preparation of the SA using only acid or base as a catalyst: The procedure for preparing the SA using only HCl or NH₄OH was followed section 3.2.2. There were some differences in the sol-gel formation step. These differences are discussed below:

3.2.4.1 Sol-gel formation using an acid catalyst

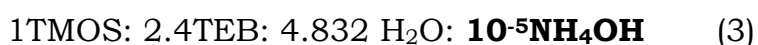
The volume of the TMOS and the volume of the H₂O were divided into two parts each (Part A and Part B) in accordance with molar ratio determined by equ. 2 (below). Part A of the TMOS was added to the TEB solvent in a beaker and stirred at 40 °C with a hot magnetic stirrer. Then, Part A of the water, as well as HCl, were added to the same beaker using continuous stirring. After

that, Part B of the TMOS was added. After 1–2 minutes, Part B of the H₂O was added to the beaker with continuous stirring for 35 minutes at 40 °C to form the sol-gel solution. The molar ratio was:



3.2.4.2 Sol-gel formation of the base catalyst

After dividing the volume of the TMOS and the volume of the H₂O each into Part A and Part B according to the molar ratio in equ. 3 (below), part A of the TMOS was added to the TEB in the beaker with continuous stirring at 40 °C with a hot magnetic stirrer for homogenisation. Then, Part B of the TMOS was added. After 1–2 minutes, Part B of the H₂O was added to the beaker using continuous stirring for 30 minutes at 40 °C. Next, NH₄OH was added to the solution under rapid stirring for 5 minutes until the pH reached 6 at 45 °C. The molar ratio was:



3.2.5 Hypothesis: When prepared with different volume/fill depths, the primary drying endpoints of the SA would increase as the fill volumes increased. This would be determined through monitoring using a thermocouple sensor.

3.2.6 Preparation different volumes of the SA and drying using the lyophilisation cycle

The following section addresses the production of SA at volumes of 2.5, 5, 8 and 10.5 ml. This was carried out as follows:

1. **Sol-gel formation:** This procedure followed section 3.2.2, except that when the sol-gel solution was formed and transferred to the vials, the thermocouple wire was put inside the vials near the centre of the bottom. The vials were then tightly capped by rubber stoppers and put in the oven.

2. **Aging:** The procedure followed section 3.2.2.

3. **Drying:** The vials of SA were pulled from the oven and the TEB solvent was removed, as was done in section 3.2.2. Next, the ends of the wire were placed inside the vial near the centre of the bottom and connected to the other side of the sensor's channel with miniature thermocouple plugs. The device included 8 channels for each cycle, but only 6 channels were connected because each volume involved a triplicate number. A thermocouple sensor (type K) was connected to the PC with a USB cable to programme the sensor's software to start recording the data every 10 seconds. The main purpose this sensor served when inside the freeze-dryer was as follows: At the ends of the two dissimilar wires, one of the junctions was known as the hot junction that measured the temperature in the vial, while the other junction was called the cold junction and maintained the reference temperatures (as shown in Figure 8). When this pair of junctions were fused together, they generated a thermoelectric effect that produced differences between the wires measured by the voltmeter (Daintith and Martin, 2010).

The difference in voltage between these wires is known as the Seebeck Effect. The Seebeck Effect involves the production of a gradient or difference in temperature along the entire length of the metal conducting wires. This generates an electromotive force—that is, a potential difference or gradient that can be produced by a specific source of electric current—which is measured by voltmeter and which automatically translates the data from the SA vials as temperature (°C), which is then plotted against the time (Duff and Towey, 2010).

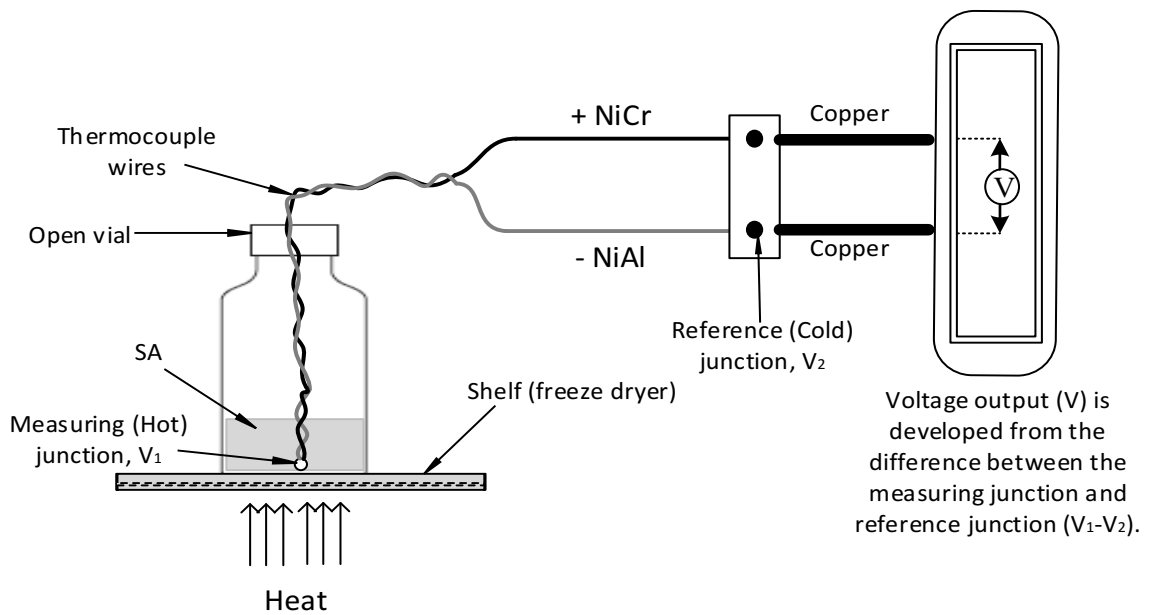


Figure 8: A schematic outline of the main work of the product thermocouple sensor undergoing the lyophilisation cycle involving vial(s), probe(s) and a thermocouple sensor (+NiCr: nickel chromium, -NiAl: nickel aluminium).

Finally, the USB cable is plugged in after the sensor has been programmed and the thermocouple is placed with the vials inside the machine to start the cycle. The cycle used in this experiment follows the procedure in Table 2. After the lyophilisation cycle is completed, the thermocouple sensor is connected to the PC2 again to automatically calibrate the data and record the temperature ($^{\circ}\text{C}$) and draw the graph (Figure 9). It should be taken into account that the freeze-dryer machine is connected to another computer (PC1) during the processing to record the cycle of the freeze-dryer, including the shelf temperature, condenser temperature and pressure.

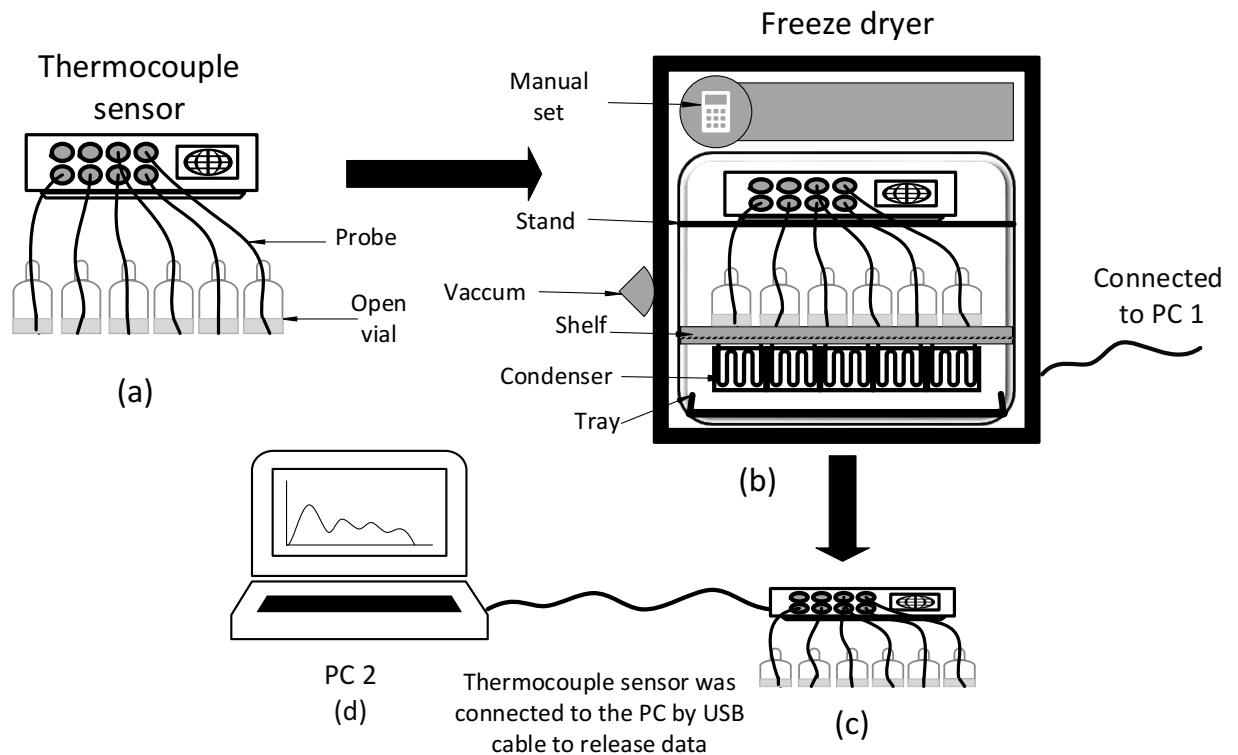


Figure 9: A schematic description of the steps to required to dry the SA sublimation of TEB from inside the sol-gel formation at 0.07 mBar, after it had been frozen at $-10\text{ }^{\circ}\text{C}$ and monitored by product thermocouple sensor **a)** Probes placed at the bottom centre of the vials using only 6 channels (as each volume being monitored was a triplicate); **b)** The start of the freeze-dryer cycle, as mentioned in Table 1, and the connecting of the machine to PC1 to record the sensor's conditions (temperature, condenser and pressure) every 2 minutes; **c)** The products collected by the thermocouples within the samples; and d) The USB cable is connected to a PC2 to translate the data that has been recorded (the temperature) every 10 seconds.

3.2.7 Hypothesis: This two-tiered hypothesis aims to investigate the effects of the AG on the duration of the primary drying of the SA; it is expected to harden the SA than the typical granules or powders.

3.2.8. Preparation of the different percentages of AG to be added to the SA and monitored by a thermocouple sensor

This procedure follows the method discussed in section 3.2.6, except for one difference in the first step:

Sol-gel formation: The volumes of the TMOS and the H₂O were both divided into two equal parts: Part A and Part B. This was done in accordance with the molar ratio in equ. 4 (below). Part A of the TMOS was added to the TEB solvent in the beaker and stirred at a temperature of 50 °C using a hot magnetic stirrer to create homogenisation. Part A of the H₂O, as well as HCl, were then added to the same beaker (Beaker 1) using continuous stirring. The AG solution was prepared by dissolving 0.25 mg of AG for every 1 ml of Part B H₂O at 45 °C for 10–20 minutes. This was done in a closed beaker (Beaker 2) with pinholes to allow for evaporation. Part B of the TMOS was then added to Beaker 1. After 1–2 minutes, the contents of Beaker 2 were poured into Beaker 1 and continuously stirred for approximately 30 minutes at 40 °C. They were not heated beyond this temperature in order to avoid transforming the AG solution into a gel during the mixing and separation.

Next, NH₄OH was added to Beaker 1 under rapid stirring for 5 minutes until the pH reached 6 at 50 °C, allowing for the obtainment of the sol-gel. The sol-gel formulation was then transferred into vials and the thermocouple wires were placed near the bottoms of these vials and tightly sealed with tissue Parafilm (M®, Nemis). Pinholes were made to allow for evaporation, and the vials were placed in the oven at 65 °C for 55 minutes in order to form the gel. The molar ratio of this experiment was:

$$1\text{TMOS}: 2.4\text{TEB}: 4.832 \text{H}_2\text{O}: 10^{-6}\text{HCl}: 10^{-5}\text{NH}_4\text{OH}, \text{ and AG}^* \quad (4)$$

*= 0.25 mg of AG was dissolved in 1 ml of Part A H₂O; because there is no specific Mwt for AG, its molar ratio could not be calculated (Creighton, 2010).

It should be mentioned that for the sake of easily following and discussing the results, each preparation following **equ. 4** was referred as **SA/AG 0.25%** (this percentage was used in the experiment).

The exact same procedure was used to prepare a larger quantity using this molar ratio:

1TMOS: 2.4TEB: 4.832 H₂O: 10⁻⁶HCl: 10⁻⁵NH₄OH, and *AG (5)
* =1 mg of AG was dissolved in 1 ml of Part B H₂O; the molar ratio of AG could not be calculated, as there was no specific Mwt (Creighton, 2010).

Also, for the sake of making the presentation and discussion easier, each preparation following **equ. 5 was referred to as SA/AG 1%** (this percentage was used in the experiment).

3.2.9. Hypothesis: The Corillonite Sensor and a microbalance can be used to determine the duration of primary drying during the lyophilisation process.

3.2.10. Preparation of SA/AG 1% and the monitoring of its sublimation using the Corillonite and microbalance sensors

The end point of the primary drying of this preparation was monitored using two sensors: the Corillonite sensor and a microbalance. This drying commenced by preparing the SA/AG 1% as discussed in section 3.2.8, aside from a difference in the aging step; for this drying process, there was no need to put the probes inside the vials. The vials containing SA/AG 1% were then removed from the oven and applied to the following sensors:

3.2.10.1. The Corillonite Sensor:

A 2.5 ml vial was collected and connected to the Corillonite sensor from one side before being placed in the centre of the middle shelf inside the freeze-

dryer. A stiff sponge was placed around the circular board for protection. The USB cable was then connected to the sensor to supply the power through one of machine's vacuums in order to begin immediately recording the data as analogue signals (10B1+ABC) per 1 second (Figure 10). Finally, the machine door was covered with tin aluminium to avoid the sensor accidentally transmitting the light as data (Badamasi, 2014). The door closed and the standard lyophilisation cycle (2.5 ml) was started, as shown in Table 2. Use of the Arduino software involved a serial monitor appearing on the computer screen, which permitted the data to be sent to and from the board. When the LED(s) on the board were flashing, it meant that the data were being transmitted through the USB cable to a chip in PC2.

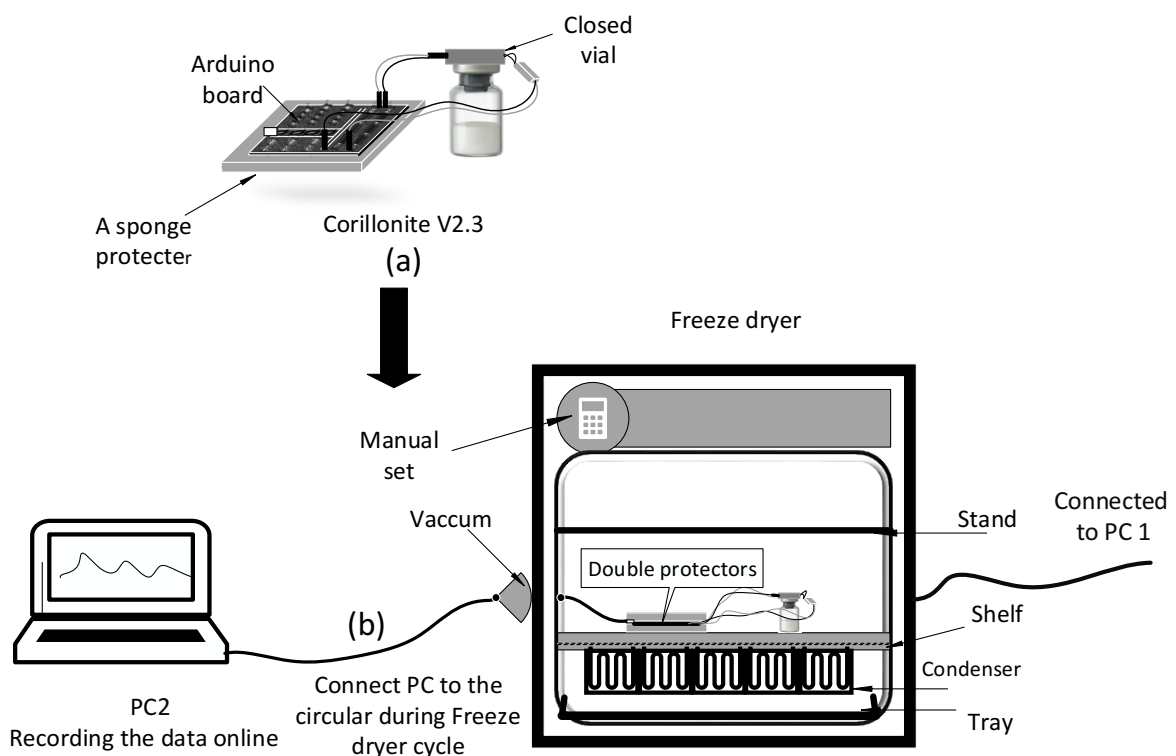


Figure 10: A schematic description of the steps required to start the drying of SA/AG 1% by sublimation of TEB from inside the sol-gel formation at 0.410 mBar, after it

had been frozen at $-10\text{ }^{\circ}\text{C}$ and monitored by Corillonite sensor, **a)** Seal the vial with the rubber stopper; **b)** At starting the freeze-dryer cycle, connect the machine to PC1 to record its conditions (temperature, condenser and pressure) every 2 minutes, then apply the sensor to the vial inside the machine and connect it to PC2 using the USB cable to translate the analogue data from the sample every 10 seconds.

3.2.10.2 *Microbalance:*

First, 20 weighted vials were filled with 2.5 ml SA/AG 1% (the solution that was prepared at beginning of this section). Then, the vials were placed in the freeze-dryer and the door was closed to start the lyophilisation cycle, as displayed below. A vial was collected every 15–20 min to be reweighed by the microbalance and without returned it to the machine:

1. The vials were frozen at $-10\text{ }^{\circ}\text{C}$ and held for at least 30 minutes.
2. The condenser was turned on until it reached -77 to $-80\text{ }^{\circ}\text{C}$.
3. The vacuum was switched on until the pressure reached 0.4–0.5 mbar.
4. Finally, the shelf control was set to $+10\text{ }^{\circ}\text{C}$ for approximately 60 min and then increased to $+20\text{ }^{\circ}\text{C}$ for 5–6 hours. When attempting to collect a vial, the vacuum pump must release to allow the door to open, and so after a vial was collected, the door had to be closed and the pressure increased again (this procedure is special for this method).

3.2.11 Hypothesis

It is assumed that SA will be hardened from the typical granules or powders when it is combined with other substances, and this might positively alter the duration of the primary drying of the SA. The sub-hypotheses are provided below:

3.2.11.1 Improving the properties of synthesised SA requires adding MAT to it.

3.2.11.2 Adding PVA to SA can produce SA/PVA products with better properties.

3.2.11.3 Adding EC to SA will produce different advantages than using native SA.

3.2.12 Preparation of different percentages of MAT to be added to SA and monitored using a thermocouple sensor

The material for this procedure follows the method in section 3.2.6 except with regards to a difference in the first step:

Sol-gel formation: First, the volume of the TMOS and H₂O were both equally divided into two parts, Part A and Part B (according to the molar ratio in equ. 6 below). Part A of the TMOS was added to the TEB solvent in the beaker and stirred at a temperature of 50 °C on a hot magnetic stirrer to be homogenised. Then, Part A of the H₂O and the HCl were added to the same beaker with continuous stirring. On another side, the MAT solution was prepared according to the molar ratio in equ. 6, and it was dissolved in Part B of the H₂O in a test tube and shaken for 3–5 minutes. After that, Part B of the TMOS was added to the beaker; after waiting for 1–2 minutes, MAT solution was poured to the beaker and stirring was continued for approximately 30 min at 45 °C to avoid separation.

Second, NH₄OH was added to the beaker under rapid stirring for 5 min until the pH became 6 at 50 °C to obtain the sol-gel. Then, the sol-gel formulation was transferred to the vials, and the thermocouple wires were put inside near the bottom and tightly sealed using Parafilm tissue. The vials were put in the oven at a temperature of 65 °C for 55 min to form the gel. The molar ratio is as follows:



It should be noted that for easily following and discussing the results and presentation, each preparation following **equ. 6** will be referred to as

SA/MAT 1% (referring to the percentage used in our experiment). Appendix 6.3.1 includes the method for calculating the MAT 1%.

Then, the same procedure was repeated to prepare a larger quantity using the following molar ratio:



Again, for easy presentation and discussion, each preparation following **equ. 7** will be referred to as **SA/MAT 5%** (referring to the percentage used in our experiment). Appendix 6.3.2 includes the method for calculating the MAT 5%.

3.2.13 Preparation of different percentages of PVA to be added to the SA and monitored using a thermocouple sensor

The method for this material follows the procedure explained in section 3.2.6 except for the difference in the first step, as shown below:

Sol-gel formation: The volume of the TMOS and the H₂O were both divided equally into two parts, Part A and Part B (according to the molar ratio in equ. 8 below). Before starting the reaction, the PVA was weighed (according to equ. 8) and dissolved in Part A of the H₂O, stirring in cold water in a test tube for 60 min (based on the PVS 87–87% hydrolysed concentration, it would be soluble in cold water (DeMerlis and Schoneker, 2003; Brydson, 2013)). First, Part A of the TMOS was added to the TEB in the beaker and stirred at a temperature of 50 °C on a hot magnetic stirrer. Second, Part B of the H₂O and the HCl were added to the same beaker with continuous stirring. Third, the PVA solution was poured into the beaker and stirred for 3 min at 45 °C. After this, Part B of the TMOS was added to the beaker, and the stirring was continued for approximately 30 min at 45 °C to avoid separation.

Finally, NH₄OH was added to the beaker under rapid stirring for 5 min until the pH was 6 at 50 °C to obtain the sol-gel. Then, the sol-gel formulation was

transferred to the vials, and the thermocouple were put wires inside near the bottom and tightly sealed using Parafilm tissue, and the vials were put in the oven at a temperature of 65 °C for 55 min to form the gel. The molar ratio was as follows:

$$1\text{TMOS}: 2.4\text{TEB}: 4.832\text{H}_2\text{O}: 10^{-6}\text{HCl}: 10^{-5}\text{NH}_4\text{OH}: 15 \cdot 10^{-6}\text{PVA} \quad (8)$$

To easily follow and discuss the results and presentation, each preparation that followed **equ. 8** will be referred to as **SA/PVA 5%** (referring to the percentage used in our experiment). Appendix 6.4 includes the method for calculating the PVA 5%.

3.2.14 Preparation of the EC to be added to the SA and monitored using a thermocouple sensor

The method for this material follows the procedure explained in Section 3.2.6 except for the difference in the first step, as shown below:

Sol-gel formation: The TEB and TMOS were prepared (according to equ. 9 below) and then to the beaker at 40 °C on a hot magnetic stirrer for 3 minutes. Second, the EC was weighed (according to the molar ratio in equ. 9), added to the beaker, and stirred vigorously until totally dissolved at 45 °C. Then, the H₂O was added to the solution; because the EC is insoluble in water due to being hydrophobic in nature, the water should be added slowly when preparing the sol-gel formation in order to avoid aggregation and separation, since both are immiscible. This was followed by adding the HCl to the solution to induce the hydrolysis, with continued stirring for approximately 30 min at 45 °C. Finally, NH₄OH was added to the beaker under rapid stirring for 5 min until the pH was 6 at 50 °C. The molar ratio is as follows:

$$1\text{TMOS}: 2.4\text{TEB}: 4.832\text{H}_2\text{O}: 10^{-6}\text{HCl}: 10^{-5}\text{NH}_4\text{OH}: 5 \cdot 10^{-3}\text{EC} \quad (9)$$

To easily follow and discuss the results and presentation, each preparation that followed **equ. 9** will be referred to as **SA/EC 5%** (referring to the

percentage used in our experiment). Appendix 6.5 includes the method for calculating the EC 5%.

3.2.15 Hypothesis

With regards to the possibility of reusing the TEB solvent, there are two hypotheses:

3.2.15.1 Reuse the ‘recycled TEB’ in preparation the aging step for new SA without affecting on its primary drying end point.

3.2.15.2 The possibility of separating the TEB from the collected liquid of the condenser.

3.2.16 Preparation of the new SA using the recycled TEB to age its structure

Preparing different volumes of SA—2.5, 5 and 8 ml—is identical to the method discussed in Section 3.2.2 except for the difference in the aging step (second step):

Aging step: After the gelation formed, the gels were immediately aged by removing the vial covers and adding **recycled** TEB (which was kept in a glass bottle during the aging step in the previous preparations, as referred to in section 3.2.2/Drying) to the SA, to strengthen the structure of the product (Su *et al.*, 2012), and the vials were immediately tightly closed to avoid crystallisation, which presumably happens because the gels react with CO₂ in the atmosphere, leading to sample cracking and solvent evaporation (Su *et al.*, 2012; Brinker and Scherer, 2013). After the vials were tightly closed, they were left between 8–20 hours in 35–40 °C to be aged.

3.2.17 The procedure for collecting the liquid condenser

After finishing the lyophilisation cycle, the condenser liquid was collected, after pressing the button to defrost the condenser, by following a simple procedure to separate the TEB from the water. 30 ml was poured into 3 separate cylinders and left in a hood for 5 consecutive days. They were not covered, and the cylinders' volumes were checked every 24 hours.

3.3 Statistical analysis

Freeze-dryer diagrams for all cycles, with the monitoring time for the primary drying for all sensors, were plotted using Microsoft Excel 2010. First, the results (the time and temperature) were plotted for all freeze-dryer cycles. Then, plotted the results of the sensors were monitored the vials drying separately, which involved triplicate samples and the Mean (Mean, SD).

After that, the primary drying time was calculated for each sample and for the Mean (curved lines in the chart) according to Figure 6, using the onset point to determine the end of the primary drying (against the time). This procedure gave four single values for the end point of primary drying: three values for the triplicate of each sample (for example, time1, time2 and time3) and one value for the Mean (Mean time).

Finally, the Mean time and SD were calculated for the plotted curved: time1, time2 and time3 values and named as '**Mean time1±SD1**' and not for all the data of samples (it means calculated the Mean and SD only for the value that resulted from plotted the temperature against the time according to the offset curve position). All the charts in the results section include the time of primary drying as "Mean time (Mean time 2±SD)". Furthermore, the statistical comparison of the data for this primary drying was done using two-way ANOVA (Sidak test for two column comparisons and Tukey test for three column comparisons) to determine the significant difference between the times of primary drying for two or three lines.

4. Results and Discussion

4.1. Results

4.1.1. Production of SA using TEB and drying with a lyophilisation process

The synthesis of SA was performed according to the methodology outlined in section 3.2.2, and the results are illustrated in Figure 11. The samples involved formed powders and granules of SA, and the latter were extremely brittle structures.

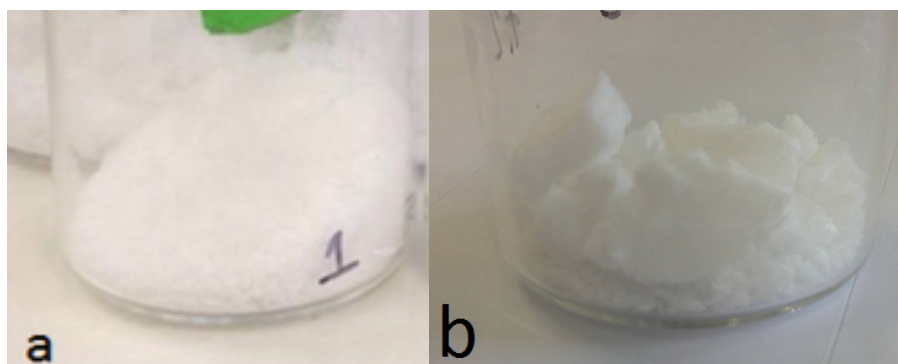


Figure 11: Photographs of native or pure SA (prepared as 1TMOS: 2.4 TEB: 4.832 H₂O: 10⁻⁶HCl: 10⁻⁵NH₄OH, equ.1) produced by sublimation of TEB from inside the sol-gel formation at 0.05 mBar after it had been frozen at -10 °C. **a)** Powder formed after drying 2.5 mL of SA, **b)** Granules formed after drying 5 mL of SA. There is no specific shape to calculate its D and H.

4.1.2. The effect of using only an acid or a base catalyst to prepare the sol-gel for SA synthesis

The attempt to synthesise SA using only one catalyst was conducted according to the procedure outlined in section 3.2.4, and the results are shown in Figure 12. It seems that the solution was unable to transform the solution mixture to gels with both formulations (a, b).

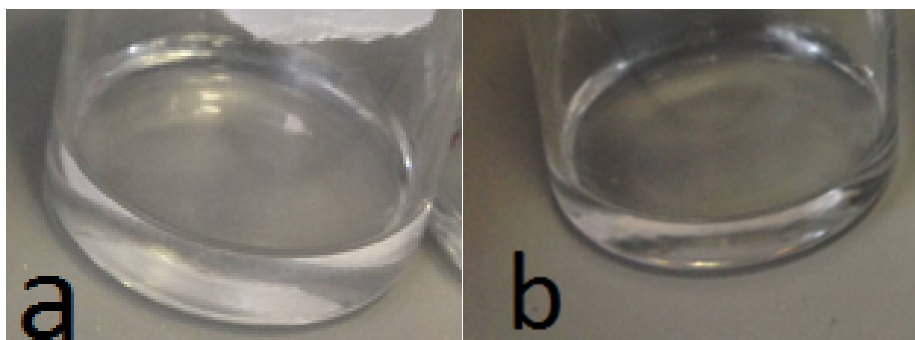


Figure 12: Photographs of the sol-gel step in the synthesis of SA using only one catalyst. **a)** Preparation involved adding NH_4OH as a base catalyst, but the sample remained a liquid and did not become a gel (prepared as 1TMOS: 2.4 TEB: 4.832 H_2O : $10^{-5}\text{NH}_4\text{OH}$ (equ.,3), **b)** preparation involved HCl as the acid catalyst, but it did not transform the solution to gels (prepared as 1TMOS: 2.4TEB: 4.832 H_2O : 10^{-6}HCl ; equ. 2).

4.1.3. Primary drying time of SA increases with increased volumes of SA

The procedure was conducted according to the method discussed in Section 3.2.6. The results of this procedure are illustrated in Figure 13. The primary drying time increases when increasing the volume of the SA vials. The **cross** lines in this figure show how the primary drying time was calculated, but they will be deleted from the following charts that show the interaction within the samples.

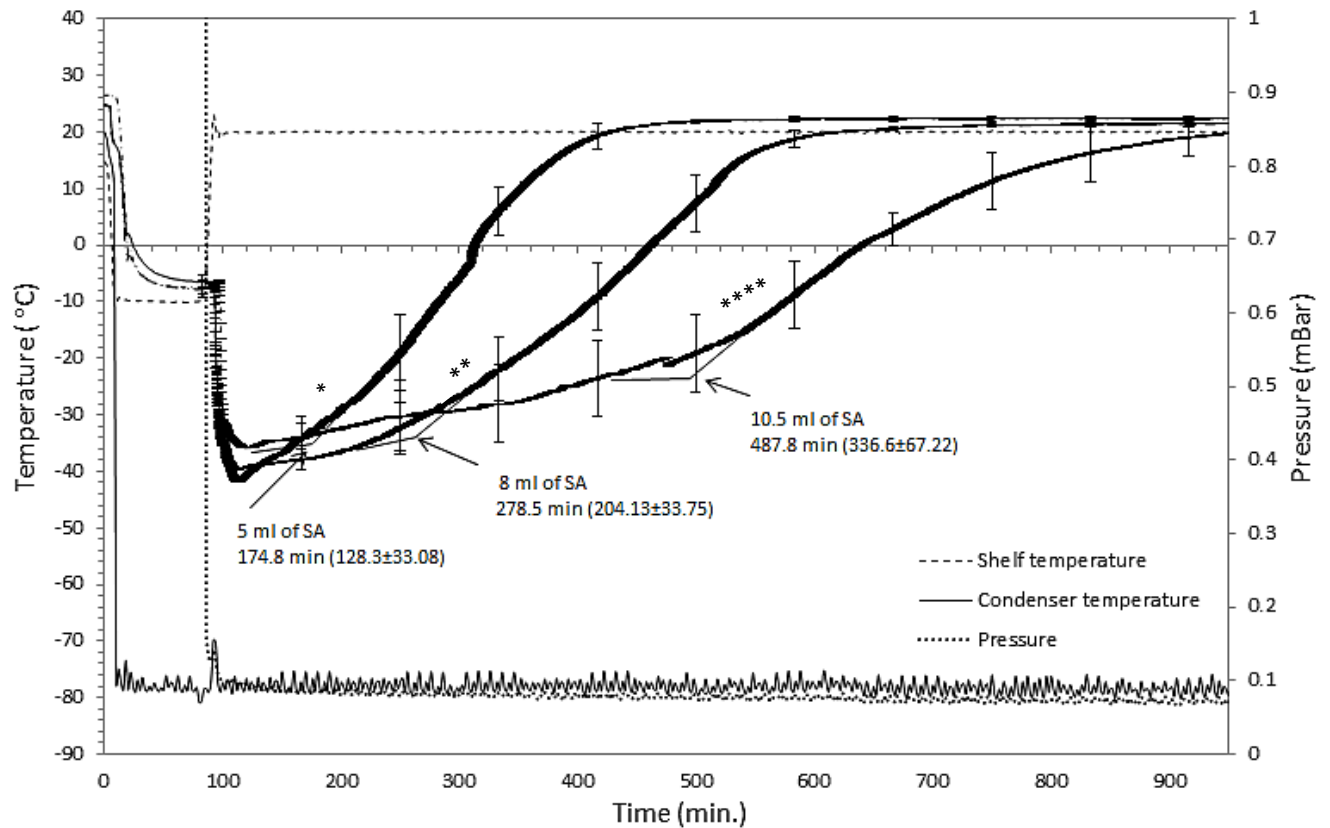


Figure 13: Chart recording the thermocouple temperatures of SA prepared as 1TMOS: 2.4 TEB: 4.823 H₂O: 10⁻⁶ HCl: 10⁻⁵ NH₄OH (equ. 1) with the probes in the centre middle inside the vials. **The two cross** lines show how to calculate the sublimation time. The arrows refer to the end point of the primary drying time for SA-produced samples using sublimation of TEB from inside the sol-gel formation at 0.07 mBar after it had been frozen at -10 °C. The D of the vial was 28 mm, and the volumes were 10.5 ml, 8 ml and 5 ml with fill depths of 25 mm, 18 mm and 12 mm, respectively. * denotes the statistical difference in the end points of primary drying between 5 ml and 8 ml ($p < 0.05$), **** denotes the statistical difference between 5 ml and 10.5 ml ($p < 0.0001$) and ** denotes the statistical difference between 8 ml and 10.5 ml ($p < 0.01$) (Mean±SD, n=3).

4.1.4. Production of SA/AG

4.1.4.1. *The effect of producing SA using AG at different concentrations during the final shaping of the product*

The method used for this material was from the methodology in section 3.2.8, and the results for the different concentrations are presented in Figure 14. The thickness (or the H) and the shape of SA/AG are more acceptable than pure SA (see Figure 11), although the hardness is not sufficient to call this preparation a cake SA/AG.

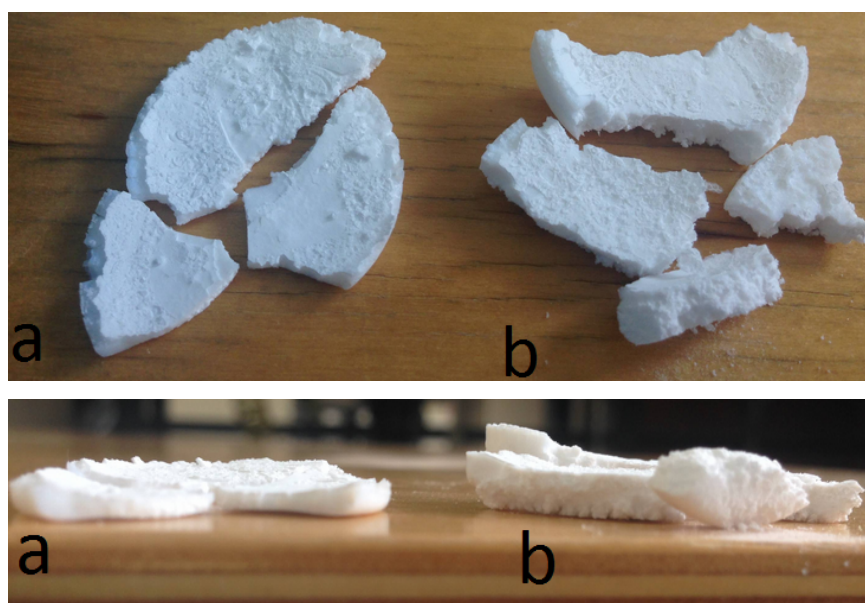


Figure 14: Photographs of SA/AG that used sublimation of TEB from inside the sol-gel formation at 0.1 mBar after it had been frozen at $-10\text{ }^{\circ}\text{C}$. They were before lyophilisation cycle with 2.5 ml, $D=28\text{ mm}$ and $H=6\text{ mm}$. **a)** SA/AG 0.25% w/v prepared as 1TMOS: 2.4 TEB: 4.832 H_2O : 10^{-6} HCl: 10^{-5} NH_4OH , and AG 0.25% (equ. 4); after drying its $H=3.5\text{ mm}$ and $D=18\text{ mm}$, **b)** SA/AG 1% prepared as 1 TMOS: 2.4 TEB: 4 H_2O : 10^{-6} HCl: 10^{-5} NH_4OH , and AG 1% (equ. 5); after drying, its $H=4.5\text{ mm}$, $D=20\text{ mm}$.

4.1.4.2. *The effect of producing SA using AG on the primary drying, monitored using a thermocouple sensor*

Figure 14 shows the results of the procedure that was presented in section 3.2.8, which confirmed our hypothesis, that SA with a larger quantity of AG could decrease the primary drying time of sublimation. Figure 14 shows the comparison of the two different concentrations of AG, which can be referred to as SA/AG 0.25% and SA/AG 1%. Moreover, Figure 15 shows the final structure for sublimation of 8 ml of SA/AG 1% for this experiment.

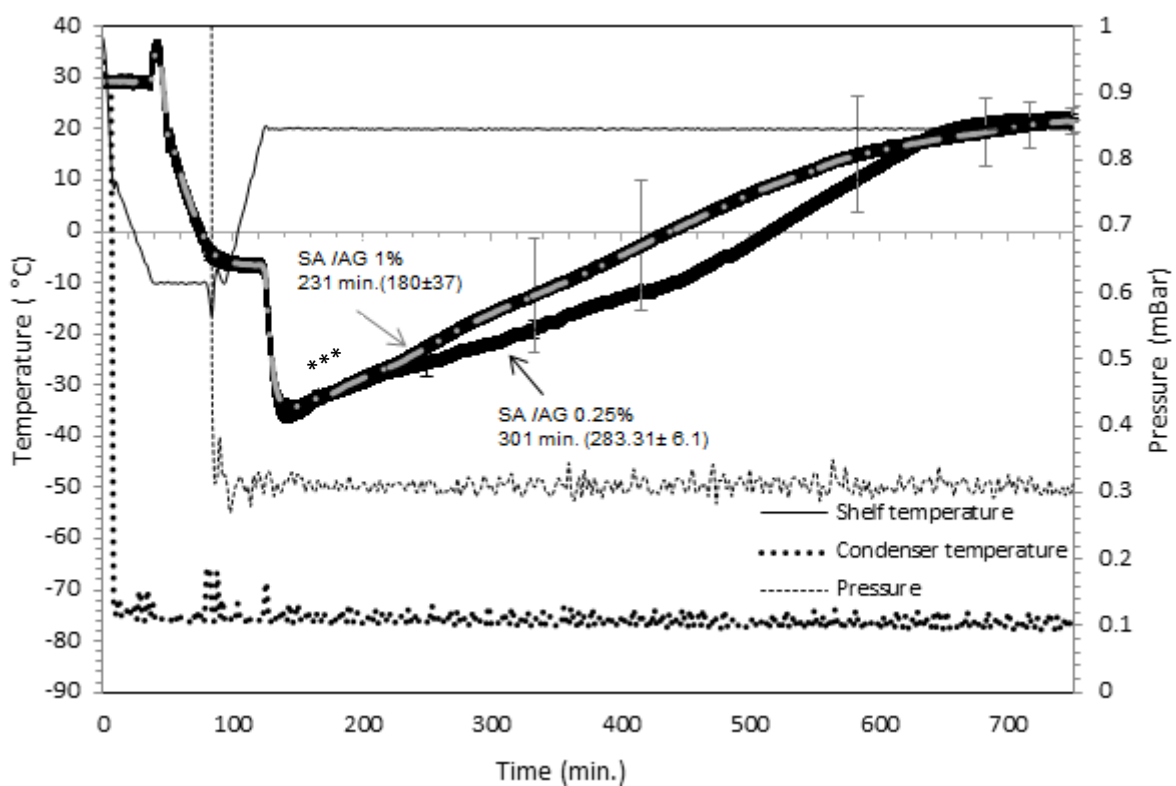


Figure 15: Chart recording the product thermocouple temperatures of the two SA/AG concentrations prepared as 1TMOs: 2.4 TEB: 4.832 H₂O: 10⁻⁶ HCl: 10⁻⁵ NH₄OH and AG0.25% (equ. 4) and 1 TMOs: 2.4 TEB: 4.832 H₂O: 10⁻⁶ HCl: 10⁻⁵ NH₄OH and AG 1% (equ. 5) (indicated % inside the figure). Arrows refer to the end point of the primary drying time for the 8 ml SA/AG produced by sublimation of TEB from inside the sol-gel formation at 0.3 mBar after it had been frozen at -10 °C in a vial with D=28 mm and fill depth=18 mm. *** denotes the statistical (p<0.001) difference between the end points of the primary drying for these samples (Mean±SD, n=3).



Figure 16: Photograph of shrinkage in SA/AG 1% (prepared as 1 TMOS: 2.4 TEB: 4.832 H₂O: 10⁻⁶ HCl: 10⁻⁵ NH₄OH and AG 1%, equ. 5) due to sublimation of TEB from inside the sol-gel formation at 0.3 mBar after it had been frozen at -10 °C. The measurement before drying were H= 25 mm and D= 28 mm, which shrunk to 14.5 mm and 24 mm, respectively, after drying.

4.1.4.3. *The effect of adding AG 1% during SA synthesis at the end point of primary drying for different volumes, monitored by a thermocouple sensor*

Figure 17 shows the results of the procedure presented in section 3.2.8. It illustrates that there is a statistically significant difference in decreasing the time of primary drying when using only 2.5 ml of SA/AG 1% in comparison with 2.5 ml of pure SA, although generally the remaining volumes of SA/AG 1% could decrease the primary drying.

Results

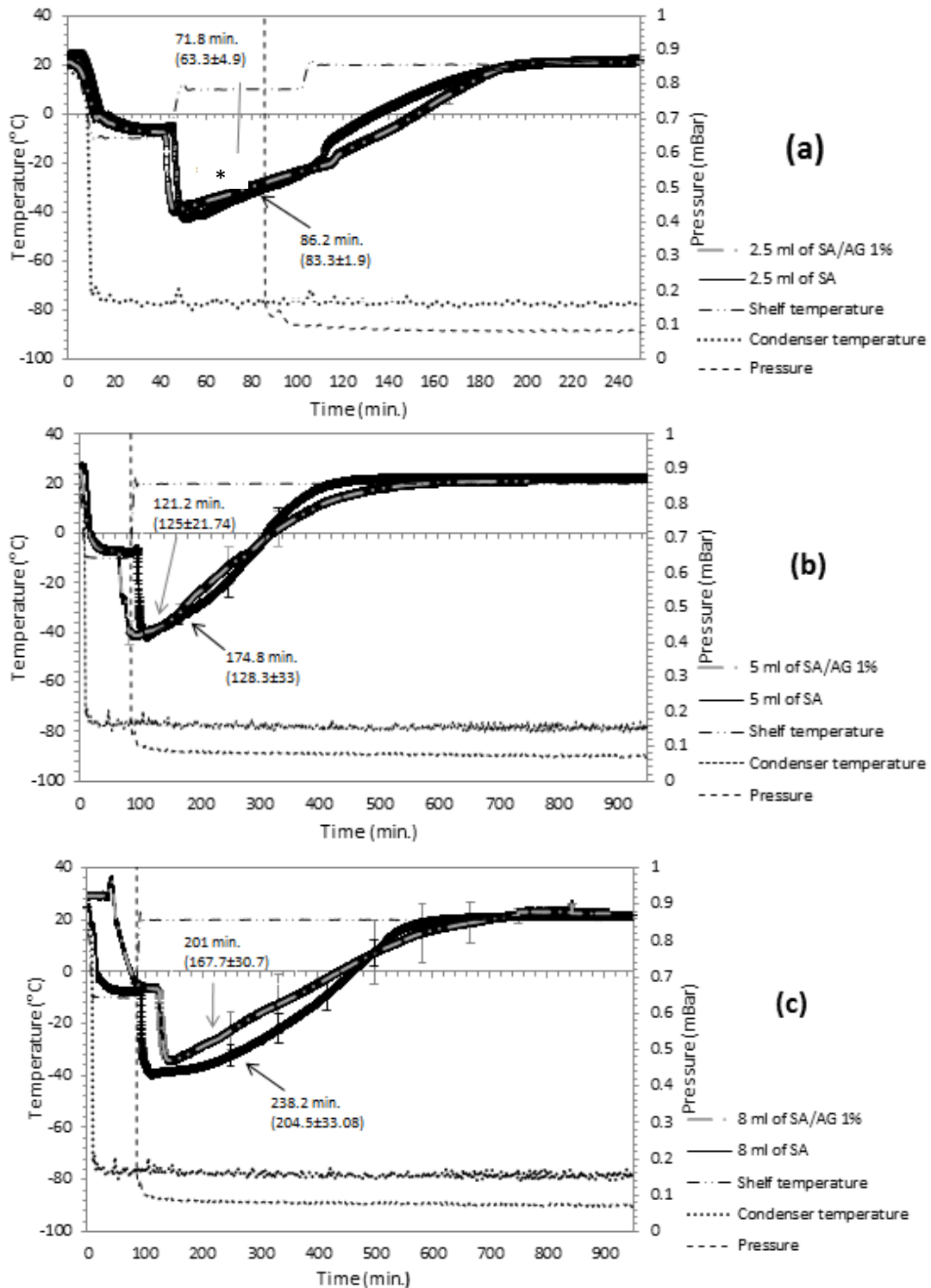


Figure 17: Charts recording the comparison of product thermocouple temperatures with the probes in the centre bottom of the vials between SA/AG 1% (prepared as 1 TMOS: 2.4 TEB: 4.832 H₂O: 10⁻⁶ HCl: 10⁻⁵ NH₄OH, and AG 1% (equ. 5) and pure SA (prepared as 1 TMOS: 2.4 TEB: 4.832 H₂O: 10⁻⁶ HCl: 10⁻⁵ NH₄OH, equ. 1). Coloured arrows refer to the end point of primary drying time. **a)** * denotes the statistical difference (p<0.05) between the end points for the primary drying of 2.5 ml of SA/AG and pure SA using sublimation of TEB from inside the sol-gel formation at 0.08 mbar for 250 min after it had been frozen at -10 °C in a vial with D=28 mm and fill depth=6 mm; **b)** end point of primary drying between 5 ml of SA/AG 1% and pure SA using sublimation of TEB from inside the sol-gel formation at 0.07 mbar for 950 minutes after it had been frozen at -10 °C in a vial with D=28mm and with fill depth=12 mm; and **c)** end point of primary drying between 8 ml of SA/AG 1% and pure SA using sublimation of TEB from inside the sol-gel formation at 0.07 mbar for 950 minutes after it had been frozen at -10 °C in a vial with D=28 mm and with fill depth=18 mm (Mean±SD, n=3).

4.1.4.5. *The effect of producing SA using AG 1% on the end point of primary drying, monitored using a Corillonite sensor*

The results were determined according to the method discussed in section 3.2.10.1. The results from monitoring with a Corillonite sensor are presented in Figure 18. It shows that the Corillonite sensor (V.2.3), by recording the analogue signals (10B1+ABC), could measure the primary drying phase, which required 74.4 min (71.4 ± 1.7) to complete the sublimation of 2.5 ml of SA/AG 1%.

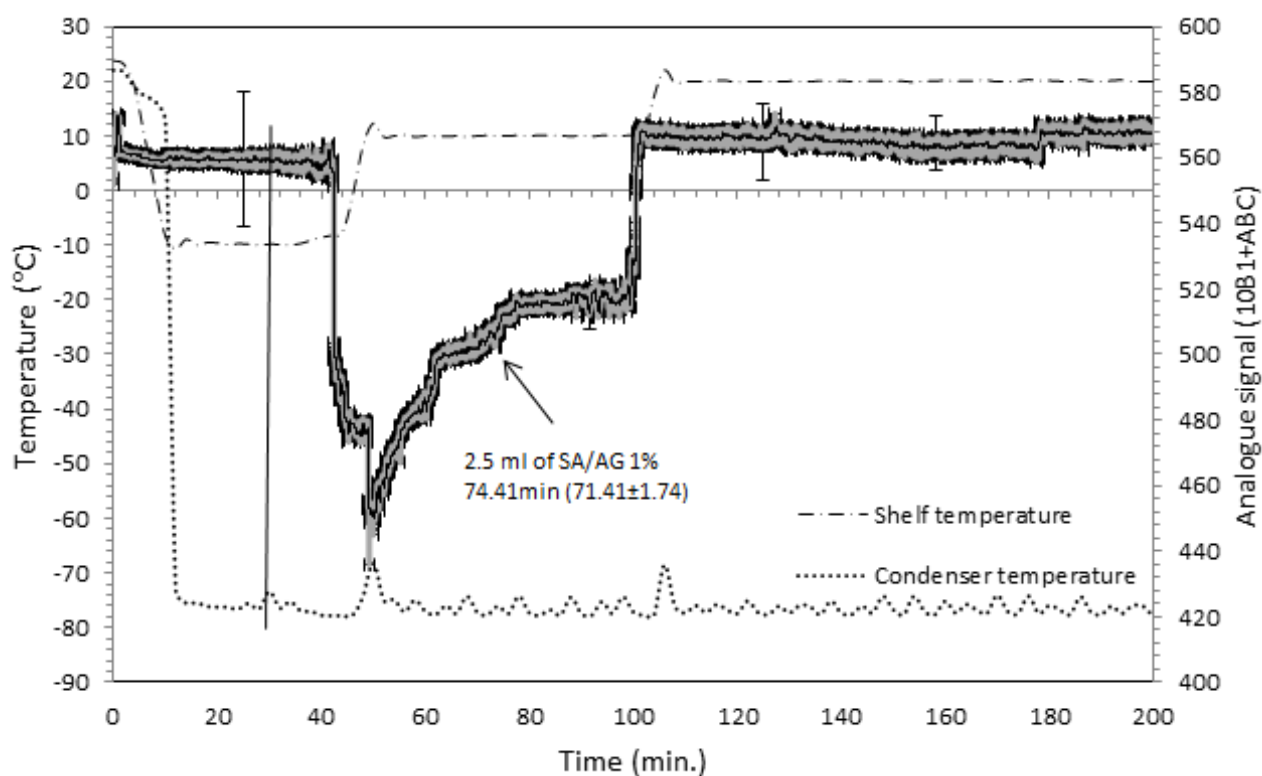


Figure 18: Chart recording the average analogue signals transmitted by the Corillonite sensor (V.2.3) **by moving average 5 points** for 2.5 ml of SA/AG 1% prepared as 1 TMOS: 2.4 TEB: 4.832 H₂O: 10⁻⁶ HCl: 10⁻⁵ NH₄OH and AG 1% (equ. 5) using sublimation of TEB from inside the sol-gel formation at 0.410 mbar after it had been frozen at -10 °C in a vial with D=28 mm, and fill depth=6 mm. The arrow refers to the end point of the primary drying phase. Vertical black line at minutes 30 represents vacuum pulldown to 0.410 mbar and is held constant. (Mean±SD, n=3).

4.1.4.6. *The effect of adding AG 1% during SA synthesis at the end point of the primary drying phase, monitored using a microbalance sensor*

The results were achieved according to the method discussed in section 3.2.10.2. The results of monitoring with the microbalance sensor are presented in Figure 19. The balance was able to measure the end point of sublimation by gradually measuring the weight loss of SA/AG 1%; the time for primary drying was 94.7 min (93.3 ± 5.7).

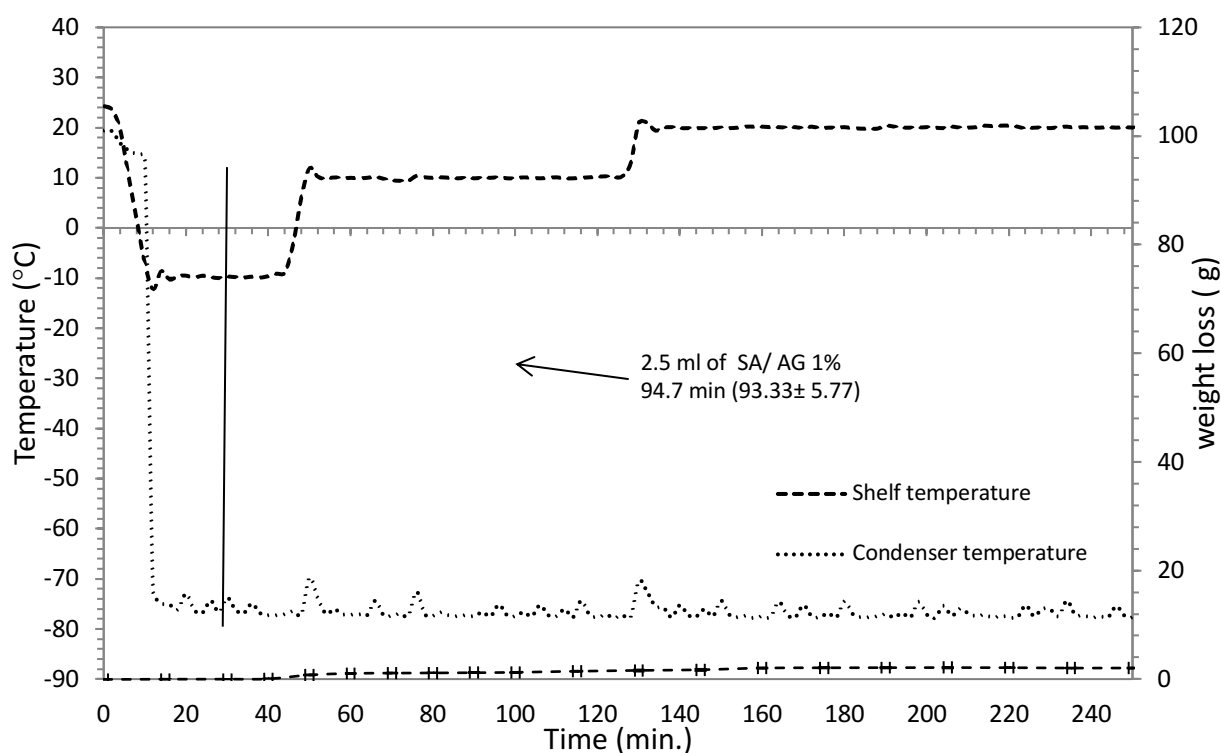


Figure 19: Chart recording the average weight loss of SA/AG 1% prepared as 1 TMOS: 2.4 TEB: 4.832 H₂O: 10⁻⁶ HCl: 10⁻⁵ NH₄OH, and AG 1% (equ.5) by sublimation of TEB from inside the sol-gel formation at 0.310 mbar, after it had been frozen at -10 °C. Arrows refers to the end point of primary drying time. **Vertical** black line minutes 30 represents vacuum pulled down to 0.310 mBar and held constant (D of the vial=28 mm, fill depths=6 mm; (Mean±SD, n=3).

4.1.5. Production of SA and MAT

4.1.5.1. The effect of producing SA using MAT at different concentrations during the final shaping of the sample

The result was achieved according to the method discussed in section 3.2.12. The results are presented in Figure 20, which shows that SA/MAT 5% could harden the shape of the formulations, especially if using a high concentration of MAT. However, SA/MAT could not form acceptable strength structure as expected.

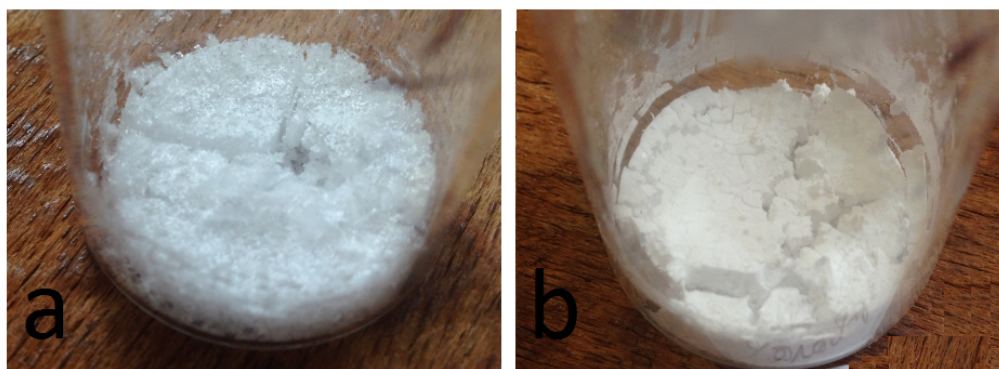


Figure 20: Photographs of SA/MAT by sublimation of TEB from inside the sol-gel formation at 0.065 mBar, after it had been frozen at $-10\text{ }^{\circ}\text{C}$. Before drying they were with 2.5 ml, $D=28\text{ mm}$ and $H=6\text{ mm}$. **a)** SA/MAT 1% was prepared as 1TMOS: 2.4 TEB: 4.832 H_2O : 10^{-6} HCl: 10^{-5} NH_4OH : $1 \cdot 10^{-3}$ MAT (referred to previously in equ.6), after drying: $H=3\text{ mm}$, $D=20\text{ mm}$, **b)** SA/AG 5% was prepared as 1 TMOS: 2.4 TEB: 4.832 H_2O : 10^{-6} HCl: 10^{-5} NH_4OH : $5 \cdot 10^{-3}$ MAT (referred to previously in equ.7), after drying: $H=4\text{ mm}$, $D=23\text{ mm}$.

4.1.5.2. The effect of adding different concentrations of MAT during SA production on the end point of the primary drying phase, as monitored by a thermocouple sensor

Figure 21 shows the results of the procedure presented in section 3.2.12. These results show the comparison between different concentrations of SA/MAT and pure SA. Using both MAT concentration 1% and 5% could decrease the primary drying when added to SA; however, two-way ANOVA

tests did not find statistical differences between this and the pure SA in terms of decreasing the end point of primary drying.

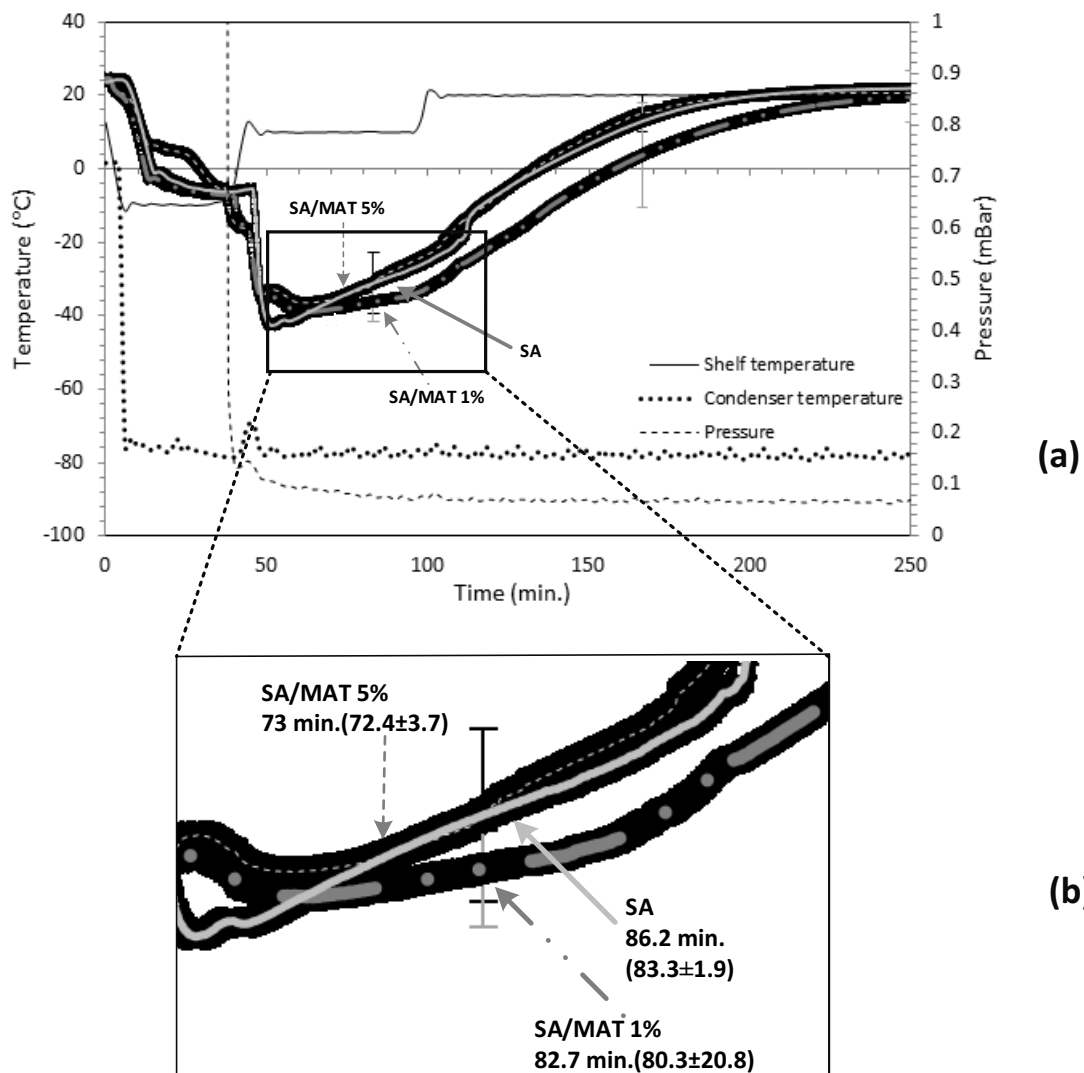


Figure 21: Chart recording the thermocouple temperatures resulting from adding different concentrations of MAT to SA. **a)** The main cycle of the three samples that included SA/MAT 1% and was prepared as 1 TMOS: 2.4 TEB: 4.832 H₂O: 10⁻⁶ HCl: 10⁻⁵ NH₄OH: 1*10⁻³ MAT (equ.6). SA/MAT 5% was prepared as 1 TMOS: 2.4 TEB: 4.832 H₂O: 10⁻⁶ HCl: 10⁻⁵ NH₄OH: 5*10⁻³ MAT (equ.7) and pure SA was prepared as 1TMOS: 2.4 TEB: 4.832 H₂O: 10⁻⁶ HCl: 10⁻⁵ NH₄OH (equ. 1.), **b)** Focused area from Figure 21a that shows the primary drying end point of the 2.5 ml samples produced by sublimation of TEB from inside the sol-gel formation at 0.07 mBar after it had been frozen at -10 °C in a vial D=28 mm with fill depths of 6 mm. The grey arrows refer to the end point of the primary drying (Mean±SD, n=3).

4.1.6. Production of SA and PVA

4.1.6.1. *The effect of using different PVA concentrations for SA synthesis during the final shaping of the sample*

The method was conducted according to the discussion in section 3.2.13. The results are presented in Figure 22. They show that PVA could harden the shape of the formulations when it was added to SA, especially if polymers with high concentrations were used. The shrinkage and cracking that occurred with SA/PVA 5% is less than that occurred with SA/AG and SA/ MAT.



Figure 22: Photograph of SA/PVA 5% (it was prepared as 1 TMOS: 2.4 TEB: 4.832 H₂O: 10⁻⁶ HCl: 10⁻⁵ NH₄OH: 15*10⁻⁶ PVA, equ.8) by sublimation of TEB from inside the sol-gel formation at 0.08 mBar after it had been frozen at -10 °C. Before drying it was with 2.5 ml, D=28 mm and H=6 mm. After drying: H=5.3mm and D=26 mm.

4.1.6.2. *The effect of adding PVA 5% during SA production at the end point of the primary drying phase, as monitored by a thermocouple sensor*

Figure 23 shows the results of the procedure presented in Section 3.2.13, which compared SA/PVA 5% with pure SA. Although there was only a 4 minutes difference between the two, a two-way ANOVA showed a statistical difference between using the polymer and using the native SA. Thus, SA/PVA 5% could shorten the end point of the primary drying.

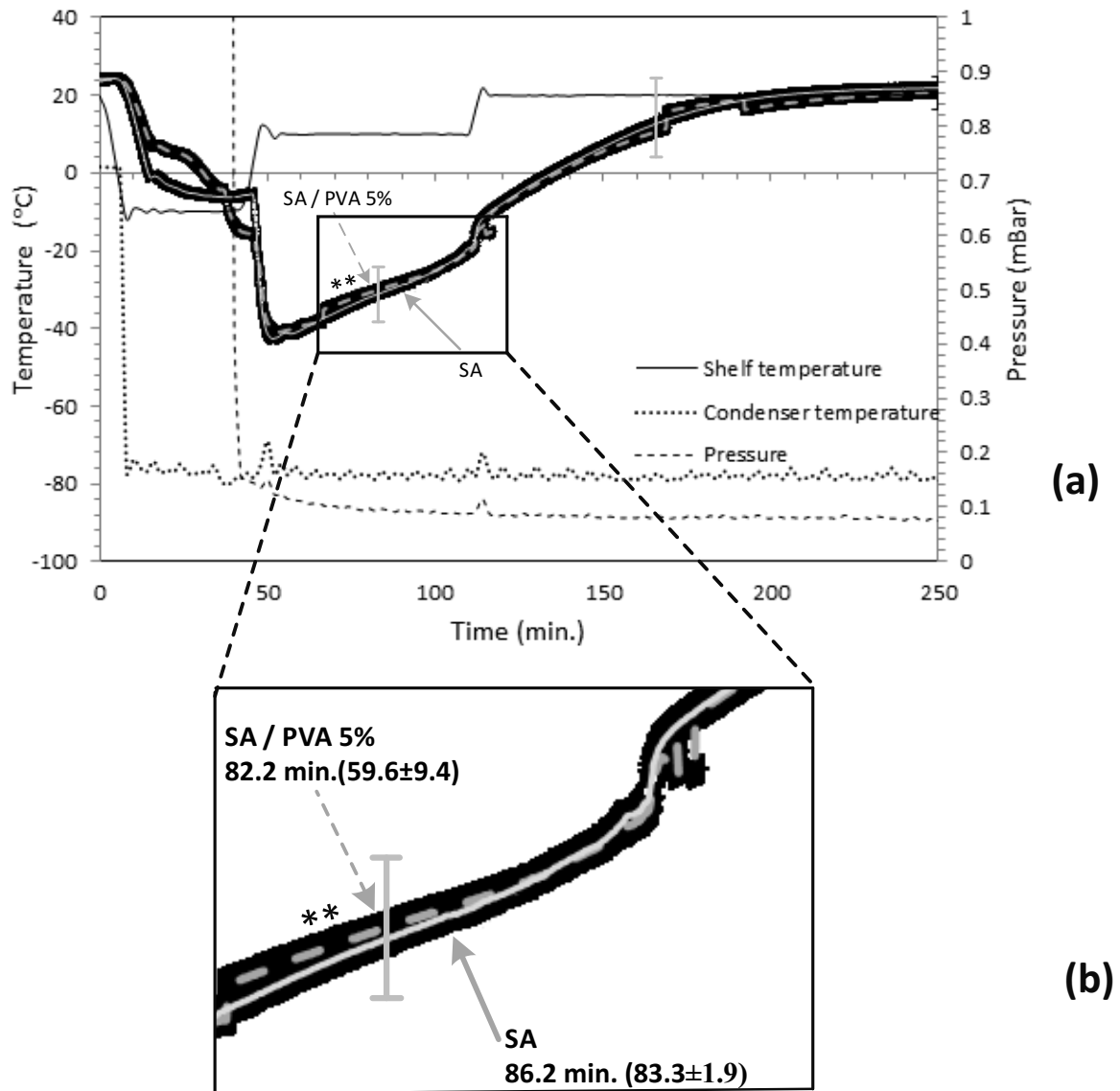


Figure 23: Chart recording the thermocouple temperatures produced by adding PVA 5% to SA. **a)** The main cycle of SA/PVA 5% that was prepared as 1 TMOS: 2.4 TEB: 4.832 H₂O: 10⁻⁶ HCl: 10⁻⁵ NH₄OH: 15*10⁻⁶ PVA, equ.8), **b)** Focused area from Figure 23a that shows the primary drying end point of the 2.5 ml samples produced by sublimation of TEB from inside the sol-gel formation at 0.08 mBar after it had been frozen at -10 °C in a vial D=28 mm with fill depths of 6 mm. The grey arrows refer to the end point of the primary drying. ** denotes the statistical difference ($p < 0.01$) between the endpoint of primary drying between these samples (Mean±SD, n=3).

4.1.7. Productions of SA/EC

4.1.7.1. *The effect of adding EC 5% to SA during the final shaping of the sample*

The method was conducted according to the discussion in Section 3.2.14. The results are shown in Figure 24. They show that EC 5% could alter the final structure of SA, creating a greater structure than that of native SA (as shown in Figure 11).



Figure 24: Photograph of SA/EC 5% prepared as 1 TMOS: 2.4 TEB: 4.832 H₂O: 10⁻⁶ HCl: 10⁻⁵ NH₄OH: 5*10⁻³ EC (equ.9) by sublimation of TEB from inside the sol-gel formation at 0.2 mBar after it had been frozen at -10 °C. Before drying with 2.5 ml, D=28 mm and H=6 mm. After drying, H=4.4 mm and D=22 mm.

4.1.7.2. *The effect of adding EC 5% during SA production at the end point of the primary drying phase, as monitored by a thermocouple sensor*

Figure 25 shows the results of the procedure presented in section 3.2.14. This procedure involved comparing SA/EC 5% with pure SA. The two-way ANOVA showed a statistical difference between using the polymer and using the native SA. Thus, SA/EC 5% can decrease the end point of primary drying.

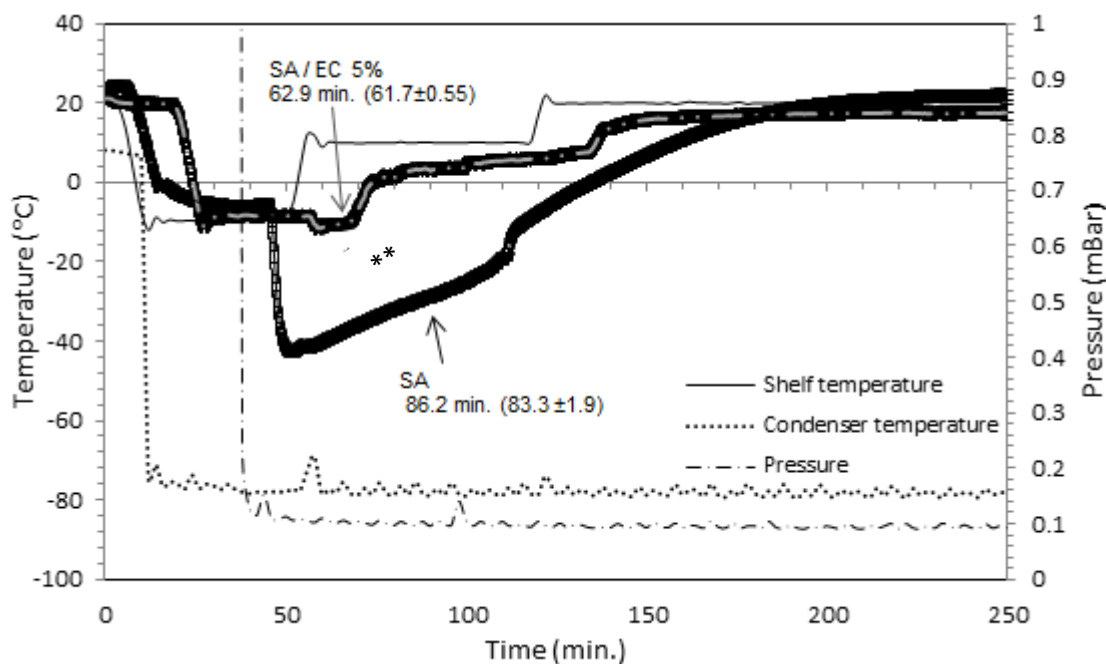


Figure 25: Chart recording the thermocouple temperatures produced by SA/EC 5%, which was prepared as 1 TMOS: 2.4 TEB: 4.832 H₂O: 10⁻⁶ HCl: 10⁻⁵ NH₄OH: 15*10⁻⁶ PVA, (equ.9). Arrows refer to the end point of the primary drying time of 2.5 ml SA/EC and of the pure SA produced by sublimation of TEB from inside the sol-gel formation at 0.1 mBar after it had been frozen at -10 °C in a vial with D=28 mm and fill depths of 6 mm). ** denotes statistical differences in the end times of primary drying between the 2.5 ml SA/EC and pure SA (p<0.01; Mean±SD, n=3).

4.1.8. The effect of preparing new SA using the recycled TEB to age its structure without affecting the primary drying end point

Section 3.2.16 explains the preparation of new SA and the use of recycled TEB for aging the new SA's structure. The results of this procedure are presented in Figure 26. A two-way ANOVA showed that there was not any significant change in the primary end point of drying between aging SA using pure TEB and aging SA using recycled TEB, meaning that any solvent used in the experiment should be kept and later reused.

Results

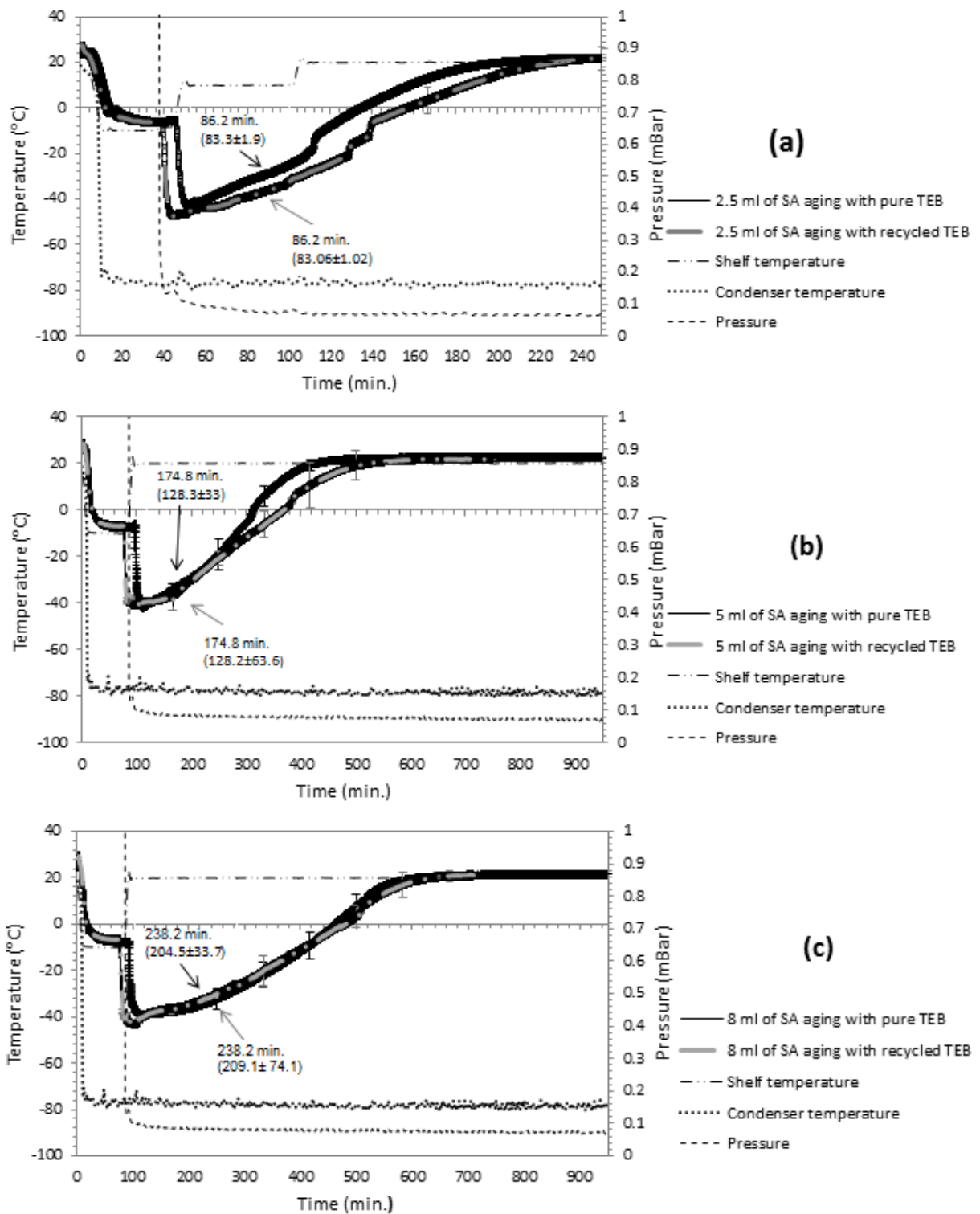


Figure 26: Charts recording comparisons of the thermocouple temperatures produced by putting the probes in the centre bottom of the vials between SA aging with pure TEB and SA aging with recycled TEB. All samples were prepared as 1 TMOS: 2.4 TEB: 4.832 H₂O: 10⁻⁶ HCl: 10⁻⁵ NH₄OH (equ.1). Arrows refer to the end point of the primary drying time: **a)** The end point of primary drying for the 2.5 ml samples by sublimation of TEB from inside the sol-gel formation at 0.07 mBar for 250 minutes. after the samples had been frozen at -10 °C in vial D=28 mm with fill depths of 6 mm; **b)** The end point of primary drying for the 5 ml samples by sublimation of TEB from inside the sol-gel formation at 0.07 mBar for 950 minutes. after the samples had been frozen at -10 °C in vial D= 28mm with a fill depth of 12 mm; **c)** The end point of primary drying for the 8 ml samples by sublimation of TEB from inside the sol-gel formation at 0.07 mBar for 950 minutes. after the samples had been frozen at -10 °C in vial D= 28mm with a fill depth of 18 mm. There were no statistical differences between any of the samples within each respective volume (Mean±SD, n=3).

4.1.9 Liquid collected from the condenser

The procedure for these results is discussed in Section 3.2.17. The results are presented in Figure 27. There was no change during the first hour in the total volume of the liquid collected from the condenser. After the first hour, the evaporated volume increased gradually before it stabilised at 20 ml after 5 days. The statistical calculation used in this experiment followed the standard method to determine the Mean and SD, unlike in the previous charts (as discussed in section in 3.3).

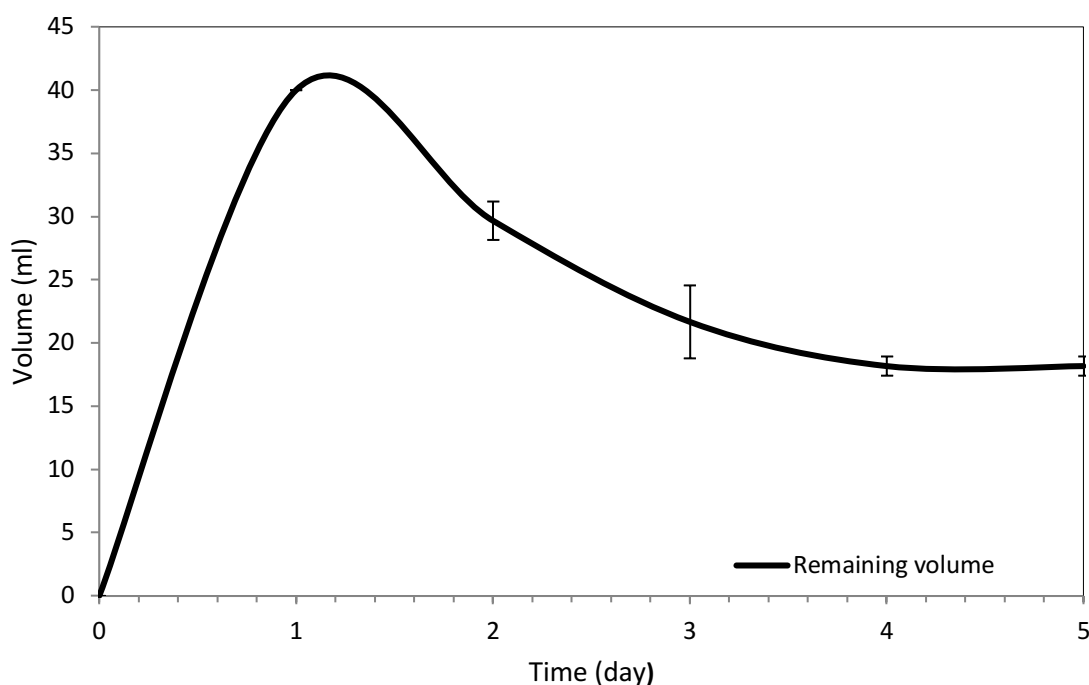


Figure 27: Chart depicting the remaining volume ($18.16 \text{ ml} \pm 0.763$) of the evaporated liquid collected from the condenser (40 ml) five days after the collection (Mean \pm SD, n=3).

4.2. Discussion

Due to the wide range of data, the results from each section of the study will be analysed separately.

4.2.1 Using the novel TEB solvent as a reaction solvent during SA synthesis

Traditional methods for producing SA include the use of several solvents, but they most commonly use methanol and ethanol (Smirnova and Arlt, 2004). However, methanol and ethanol are not ideal for the production of SA by freeze-drying process, as their freezing points are too low (methanol $-94\text{ }^{\circ}\text{C}$ and ethanol $-117\text{ }^{\circ}\text{C}$) and their sublimation rates require very long cycles (Egeberg and Engell, 1989). TEB solvent is a better option for freeze-drying, since its freezing point is $-10\text{ }^{\circ}\text{C}$. For this reason, all of the lyophilisation cycles in used in this study involved freezing the samples at $-10\text{ }^{\circ}\text{C}$. Although this solvent is expensive, it has many merits. Like the traditional solvents used to prepare gels, this solvent can quickly homogenise TMOS for dissolution. It also allows for gelation in only 50–55 minutes, while all other solvents require at least 67 minutes for gelation (Smironva and Alrt, 2002).

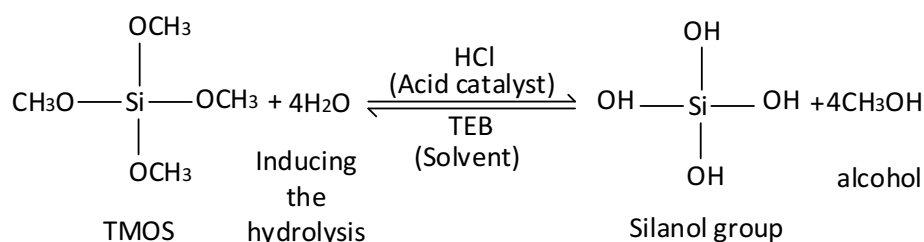
Moreover, the use of this solvent allows for elimination of the solvent exchange process. This step is typically used in commercial SA production for drying the medium by evaporation when the reaction solvent (e.g., ethanol) has a freezing point of less than $-18\text{ }^{\circ}\text{C}$ and is being used in conjunction with another solvent with a higher freezing point (e.g., tert-Butyl alcohol). The two solvents are exchanged with one another, and this exchange is repeated 3–5 times to decrease the ethanol concentration as much as possible. This is done to avoid boiling during the low-pressure point of the lyophilisation cycle. Because this extensive process is not required with the use of TEB, the synthesis time is reduced (Edgebere & Edgell, 1989; Su *et al.*, 2012). Moreover, TEB can also be successfully recycled (it will discussed later in section 4.2.7).

4.2.2. Using specific components and conditions in the methodology

Figure 28 explains the reasons for the use of each substance used in the Methodology. TMOS was used in all preparations because it has a common formula $\text{Si}(\text{OR})_4$ which is a precursor for the synthesis of SA. The catalysts (acid and base) were used together because each one plays a specific role in the reaction. HCl was used as an acid catalyst to induce TMOS hydrolysis (any protic acid would work for this purpose) and NH_4OH was used as a base catalyst for polycondensation to take place irreversibly. In other words, the catalysts accelerated the reaction between the components of the SA. SA syntheses require a solvent and reaction completed by three basic steps: sol-gel formation, aging and drying (Smirnova and Alrt, 2004; Su *et al.*, 2012).

TEB was used in the synthesis of SA to avoid separation in the liquid-liquid phase during the hydrolysis reaction (i.e, during the initial immiscible stages between water and TMOS) and to control the effects of silicate concentrations and water on the gelation process. The hydrolysis reaction (see Figure 28) by-product produced alcohol that could be mixed with both immiscible components, but the amount of alcohol was insufficient to complete this reaction (Brinker and Scherer, 2013).

1) Hydrolysis stage: replaces alkoxide groups (OCH₃) with hydroxyl group.



2) Condensation stage: including the silanol groups produce siloxane bonds plus water.

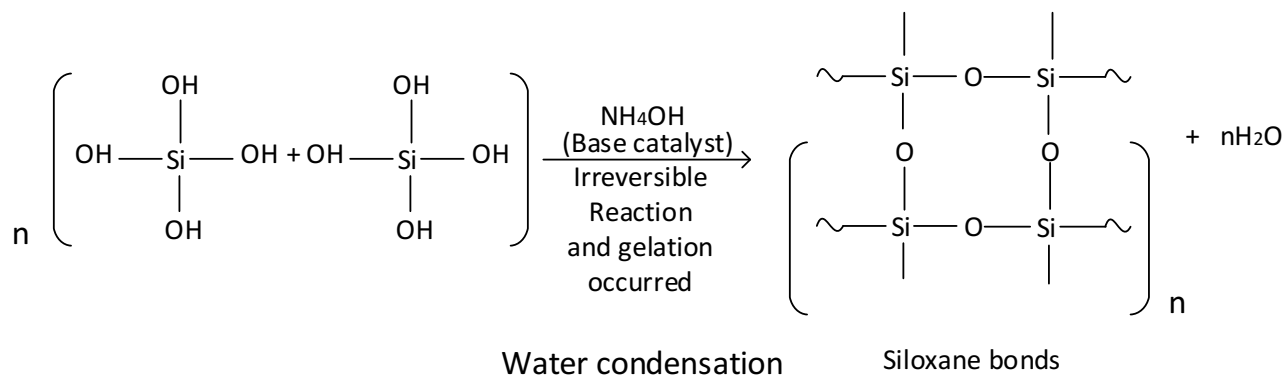


Figure 28: Schematic of the production of SA using the TEB solvent (minus the drying step). This figure depicts the purpose of using each substance. **1)** The hydrolysis stage forms silanol groups; **2)** The condensation stage forms the gelation phase (adapted from Maleki *et al.*, 2013).

Gelation and aging also play crucial roles in SA synthesis. Gelation is the growth of clusters that occurs when molecules aggregate until their clusters link and collide (also known as post-gelation), while aging helps decrease SA fracture and strengthens the networks of final SA by increasing the connections amongst SA particles (also known as additional cross-linking) during aging with the TEB (Haereid *et al.*, 1995). In fact, there are various mechanisms might happen simultaneously (but at different rates) during the aging process, to strengthen SA structure. First, the neck growth mechanism includes the reprecipitation of silica dissolved from its original location, on the surface of the product, to the necks of the particles (specifically, between the secondary particles). Second, Ostwald ripening involves the dissolution of small particles of SA compounds and precipitation onto bigger ones (Strøm *et al.*, 2007; Estella *et al.*, 2007; Maleki *et al.*, 2013). Moreover, Brownian motion

will bring the particle clusters in contact and reaction with each other, and increase the number of siloxane bridges (connection points). This reinforces and strengthens the neck regions of the SA network (Bisson et al., 2003).

It should be mentioned that no change to the strength of the SA occurs if aging has occurred for more than 20-48 hours, which is why the aging in the present study lasted for approximately 24 hours (Smirnova and Alrt, 2004; Pons *et al.*, 2012). However, some researchers prefer to avoid gelation and aging if the gelation substance will immediately dry by freeze-dryer process, as aging may increase the possibility of shrinkage during drying.

In regard to the molar ratio of H₂O, using 2 molars is insufficient for inducing the hydrolysis of TMOS in the first stage. Although increasing the water volume can accelerate the reaction, a molar ratio of more than 10 will slow the condensation stage down, as this ratio leads to the completion of the hydrolysis reaction before the condensation stage has happened; both of these events should occur concurrently. Media levels of 4–5 were therefore used in this case to control the hydrolysis and condensation reactions that would have led to decreases in gelation time (making gelation time less than 12 hours; Brinker and Sherer, 2013).

In addition, when the pH was less than 2, the gelation time always required several days to reach completion. A pH of 6 was a more appropriate value for these experiments, as this pH decreased the sol-gel formation time to be approximately 17 hours. Although pH > 7 had a greater stability effect on SA, this value required using a greater base catalyst ratio, which may have led to changes in the SA's final properties. Moreover, if the vials had been placed on the edge of the shelf, they would have dried faster than those placed in the middle of the centre shelf, as the outer vials would have had greater exposure to radiation from the door and walls of the chamber. Therefore, a 10–20%

increase in the soak period would have been required to compensate for the vials being placed on the edge of the shelf. To avoid this problem, all vials were placed in the centre of the middle shelf (Patel *et al.*, 2010; Brinker and Sherer, 2013; Fissore, 2013).

4.2.3. Explanation of the results of preparing SA using one catalyst

Mizuno *et al.* (1988) found that SA drying could be accelerated if SA were soaked in HCl or in NH₄OH. Tamaki and Chujo (1998) prepared silica gel by hydrolysis using only HCl. In the present study, however, producing SA using TEB as a solvent with adding only acid or base did not result in a forming gelation phase (see section 3.2.4, section 4.1.2 and Figure 12). This was presumably because the aging time for using only HCl should be 92 hours and the aging time for using NH₄OH should be 107 hours, while the aging time used for this experiment was approximately 20-24 hours (using standard procedures for all preparations for accurate comparison of the results).

4.2.4. Increased volumes lead to increased primary drying times

Section 4.1.3 includes the results of drying SA by freeze-dryer (see section 3.2.6). There was a significance difference between the duration of the primary drying for several volumes when the volumes/fill-depths of SA were changed, as shown in Figure 13. The smallest volume (5 ml) of SA required less time to reach the ending point of the primary drying than the 8 ml and 10.5 ml volumes with fill depths of 12 mm, 18 mm and 25 mm, respectively. This variation occurred because the vapour flow rate was reduced by the high fill depths/volumes, which increased the time required for primary drying when increases the fill depths of the vial. Thus, the temperature required to sublimate these products should be increased with increases in the fill depth of SA (Schneid and Gieseler, 2008; Brinker and Sherer, 2013). However, because all of the samples with different volumes were applied within a

standard cycle (shelf temperature=20°C), there were led to this variations in the primary drying time.

It was also observed that for this cycle (Figure 13), as well as for the SA/AG, SA/MAT and SA/PVA cycles, during the sublimation phase when the temperature shifted from -10 °C in the freezing phase to 20 °C for sublimation, the thermocouple probes recorded decreases in the temperature for these products (dropped to -30 to -45 °C). Unfortunately, there is not enough existing research to support the significance of this observation, as this is the first time to notice TEB behaviour during the freeze-drying cycle. It can be assumed that the TEB solvent absorbed the heat from the shelf and used it to create energy to achieve the sublimation process, thus resulting in the drop in SA temperature. This can be considered an exothermic reaction. This reaction may be considered an advantage of the TEB solvent, as it enables the solvent to be used for chemical applications requiring high levels of energy. However, further research using TEB with different formulations and cycles is required to confirm this exothermic reaction.

4.2.5. The effects of adding AG to SA formulations

4.2.5.1 Production of SA/AG samples

AG is a cheap substance, and it requires high temperatures to be soluble in water; otherwise, it forms reversible gels. AG concentration range of 0.2–1% is recommended for use with different preparations to strengthen the media (Djabourov *et al.*, 2013). Figure 14 shows how AG has changed the final appearance of SA after it has created a powder (see section 3.2.8). This presumably occurs because AG has the ability to form double helices and then aggregate those helices into bundles. When it is added to a solution, it creates stiff bridges between the particles. Some authors say this occurs because of the sulphated form inside the AG composition (Figure 29). The concentration of AG has a crucial effect on its strength. That is, the AG

strength increases as the concentration increases, as seen in the results (Figure 14), which show that SA/AG 1% has more strength to its shape than SA/AG 0.25% (Bronzino and Peterson, 2014). It was not possible to use a stronger concentration in our experiment because the solubility was decreased when the AG was added to the hydrophobic solution.

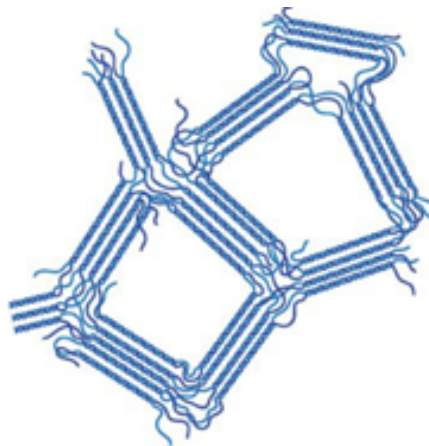


Figure 29: Schematic representation of the AG network structure composed of bundled helices (Djabourov *et al.*, 2013).

4.2.5.2 *The effect of AG on the primary drying time of SA as determined by thermocouple temperature*

The results of AG 0.25% and AG 1% were compared in regard to faster drying time and different SA volumes. The results from the thermocouple sensor (Figure 15) indicate that 8 ml of SA/AG 1% dried significantly faster than SA/AG 0.25%. There are a few possible explanations for these variations. First, the small pore size of AG largely increases with increases to its concentration, specifically $> 0.4\%$ w/v, which increases the vapour flow that escapes from AG 1% (Djabourov *et al.*, 2013). Second, Schneid and Gieseler (2008) determined that vapour flow increases with increases in concentration (or solid content) of identical vials (i.e., identical in fill depth, diameter and volume), which leads increases in sublimation.

AG 1% has a significantly faster primary drying time than other volumes of pure SA (2.5, 5 and 8 ml). The preparation of this solution was detailed in section 3.2.8, and the results were presented in Figure 17. Although all volumes of SA/AG 1% decreased the primary drying time compared to the time required for pure SA, only the 2.5 ml sample of SA/AG 1% had statistically significant difference from the 2.5 ml sample of pure SA. Therefore, 2.5 ml of SA/AG 1% was monitored with the remaining sensors because of its faster primary drying time, which made it more cost-effective (see section 1.2, which discusses the goal of minimising freeze-dryer costs by decreasing primary drying duration).

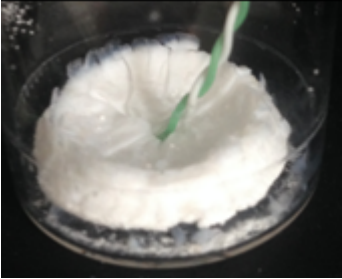

4.2.5.3 *The efficiency of the sensors for measuring the end point of the primary drying time of SA/AG 1%*

As mentioned in section 9.5.2, a thermocouple temperature sensor can measure the primary drying point of products with different volumes. As seen in the results presented in section 4.1.4.5 (which report on the procedure from Section 3.2.10.1), the Corillonite sensor monitored the time of sublimation through the transmittance of the analogue signal from the sample (as shown in Figure 18). Additionally, as seen in Figure 19 (section 4.1.4.6), the microbalance sensor monitored the sublimation time of 2.5 ml of SA/AG 2.5% when it weighed the 20 vials separately (as discussed in the procedure reported in section 3.2.10.2). There was a significance difference in sublimation time between these sensors, as well as a difference in how the sensor dealt with the samples (see Table 2).

Generally, the thermocouple sensor can be considered the most important parameter for measuring product temperature because it is nontoxic, precise, cost-effective and easy to manufacture. It measures a wide range of temperatures, in particular type k (see Appendix 6.1 for the properties of the thermocouple sensor), which encompasses temperatures between -200°C and 1260°C (Wang *et al.*, 2013; Hung *et al.*, 2005). Moreover, the thermocouple

device can monitor a group of vials together in one cycle (see Figures 5 and 9). However, as shown in Table 2, the thermocouple sensor is an invasive device. When its probes are applied inside the vials, has some disadvantages.

Table 2: Main variations between devices used to measure the end point of primary drying for 2.5 ml of SA/AG 1%.

Device	Primary drying time (Mean ± SD)	Sample shape during monitoring
Thermocouple sensor (8 channels)	86.2 minutes (83.3±1.9)	
Purpose	Measuring the change in temperature	
Number of vial run for each cycle	8 vials ^a	
Corllonite sensor (V.2.3)	74.41 minutes (71.41±1.74)	
Principle of work	Recording the signal analogue data	
Number of vials run for each cycle	1 vial	
Microbalance	94.7 minutes (93.33±5.77)	The sample was weighed outside of the freeze-dryer machine
Principle of work	Measuring the residual weight loss	
Number of vials run for each cycle	No limit	

^a= Only 6 vials were used in the present study because each sample was measured as a triplicate number for a specific volume.

First, the thermocouple sensor requires a special technique to set up its probes at the centre of the vials, as the wires of these sensors are very soft and easily moved. Second, penetration of the sample by the wires may destroy the sample's structure when the wires are removed after the cycle has

finished. Moreover, the wires act as a crystallization point in the freezing phase of the lyophilisation cycle, which may affect the heat conduction during the sublimation or drying of the product (Roth *et al.*, 2001). Additionally, thermocouple sensors have limitations if used in corrosive or harsh environments.

The Corillonite sensor, on the other hand, is a non-invasive device, meaning that it will not cause damage to the structure of the sample (Table 2). However, it is more expensive than other sensors because it is difficult to manufacture and it can only deal with one vial at a time (Figures 7 and 10) (Batmasia, 2014). The microbalance sensor is available in every laboratory, it is a cheap device and it easily measures SA/AG 1%. Still, the microbalance sensor may lack of accuracy, as it measures the samples outside the freeze-dryer, unlike like the other sensors which measured the samples while they are still on the freezer shelf (Roth *et al.*, 2001). These differences in the types of sensors may partly explain the variations in estimated times of primary drying for the same samples.

4.2.6 The effects of different substances on SA

4.2.6.1 *The effects of using MAT during SA*

4.2.6.1.1 The effects of MAT on the structure of the product

Figure 20 (a, b; Section 4.1.5) shows the final appearance of SA/MAT with different concentrations. This was conducted using the procedure from section 3.2.12. Although both photographs show an inelegant hardened shape, the shape of SA/MAT 5% is more acceptable. MAT was added because it works as a bulking agent in the lyophilisation process. It crystallises easily to form an elegant and rigid cake product. Moreover, MAT has a high eutectic temperature. In fact, eutectic point is the lowest temperature possible for a crystalline substance to exist in a liquid phase in equilibrium with a solid phase in the same system (Adams, 2007): -2.2 °C (Mehta *et al.*, 2013) or -1.4

°C (Ward and Matejtschuk, 2010). This temperature leads to simple and fast primary drying. Any temperature greater than the MAT eutectic point leads to a collapse of the product and cannot produce a cake (Passot *et al.*, 2010). This is why a collapse occurred in this formulation, as the freezing phase during the SA/MAT lyophilisation cycle was set at -10 °C (see Figure 21).

4.2.6.1.2 The effect of adding MAT on SA primary drying times, as determined using the thermocouple temperature

Figure 21 (Section 4.1.5) shows the results of the procedure presented in Section 3.2.12, wherein the thermocouple sensor monitored the primary drying temperature of SA, SA/MAT 1% and SA/MAT 5%. The results indicate that the primary drying of SA/MAT 5% is faster than that of SA/MAT 1% and pure SA; the times were 73 minutes (72.4 ± 7), 82.7 minutes (80 ± 20.8) and 86.2 minutes (83.3 ± 1.9), respectively. This variation likely occurred due to the annealing effect. The annealing effect can be defined as holding the product isothermally at a point below the eutectic temperature (-1.4 °C) and above the glass transition temperature. The latter temperature is related to the amorphous substance, which is the temperature where the vitrified residual liquid occurs in the presence of ice (Tan *et al.*, 2007; Searles, 2010; Dietrich *et al.*, 2010).

It was observed that SA/MAT 1% was fully collapsed (as mentioned in section 4.2.6.1.1), meaning that the high crystals grown during this step impeded the flow of the vapour by increasing the dry layer of crystals; hence, the product required more time to complete the sublimation. Regarding the more acceptable shape of SA/MAT 5% (see Figure 20), it was assumed that the product was partially collapsed and that large channels were formed inside the product to allow the water vapour to escape more easily (Adams, 2007; Searles, 2010; Ward and Matejtschuk, 2010; Mehta *et al.*, 2013;). These assumptions all require further study, since current research regarding

SA/MAT synthesis using TEB is insufficient. However, there is no benefit to using MAT with any concentration to decrease the primary drying phase, as there is no statistically significant difference between the concentrations in comparison to pure SA.

4.2.6.2 *Effects of adding PVA to pure SA on the primary drying time using the thermocouple temperature*

Polymers were found to be effective for strengthening the structural network of SA and were expected to improve the mechanical properties of SA by connecting particles through hydrogen bonding, van der Waals forces or electrical forces between the organic and inorganic components of the system (Malek *et al.*, 2013). According to the procedure discussed in section 3.2.13 and the results illustrated in **Figure 22**, adding PVA to SA created new formulations with limited cake shaping because PVA, as an organic polymer, contains polar groups (hydroxyl groups; see Figure 30). These groups predictably connect to silanol groups and result from hydrolysis and condensation of inorganic precursors, such as TMOS (Figure 28), to produce strong secondary interactions (Bandyopadhyay *et al.*, 2005; Maleki *et al.*, 2013). That made the SA/PVA a tougher and stronger product than pure PVA.

Nevertheless, because of the weak bonds in the polymer-SA and the possibility of leached PVA from the SA pores during the aging step (see section 3.2.13), the strength of the SA was decreased and did not produce an elegant shape (Novak *et al.*, 1994; Gould *et al.*, 2008). The high polarity of PVA and the strong interactions of its bonds and particles (Figure 30) allowed the matrix of SA to negatively aggregate the polymer and affects its final shape (Maleki *et al.*, 2013). A few studies evaluate the behaviour of PVA when it is combined with SA during freeze-drying process, regardless of the solvent reaction used. For example, Hassan and Peppas (2000) pointed out that an increase in the sublimation time (evacuation time) of PVA during the lyophilisation cycle led

to an increase in the tensile strength. They believed that allowing a long evaporation time for PVA would strengthen the gel structure by reducing the number of imperfections or impurities, which may not be attached to the PVA network structure. Moreover, the tensile force is significantly affected by the aging process, since an increase in the latter (more than one month) resulted in increased PVA tensile strength (Hasan and Peppas, 2000). Considering these explanations, the PVA requires a special sublimation cycle and aging process time to produce an acceptable, stiff, and strong SA/PVA structure.

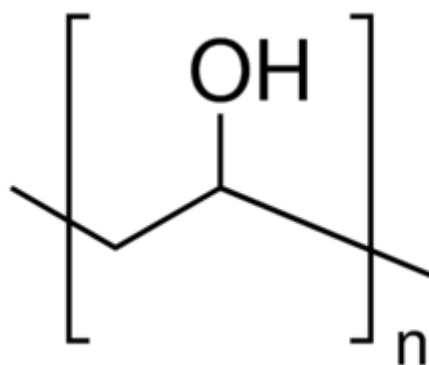


Figure 30: The chemical structure of PVA showing the hydroxyl functional group (adapted from Brydson, 2013).

The second part of the investigation involved determining the effect of SA/PVA on the primary drying time and comparing the results with pure SA. Based on the procedure outlined in section 3.2.13 and the results presented in section 4.1.6.2, Figure 23 shows that 2.5 ml of PVA/SA 5% reached the end point of the primary drying time faster than pure SA was able to, according to sample monitoring using a thermocouple device. Additionally, a two-way ANOVA analysis showed statistically significant differences between the end point of the primary drying for PVA/SA 5% and the end point for pure SA. In general concept of using the polymers, whenever a polymer is added to any formula, the strength and density of the product increase. This leads to a

decrease in the surface area of SA and decreased evaporation as a result of delayed drying times (Murtaza, 2012). The results of this experiment opposed this concept, because the SA/PVA 5% was sublimed first. As mentioned in section 4.2.4, this process was observed while the product underwent the freeze-drying process, when the escaped vapour flow increased as the concentration increased (or increased its solid content), leading to a shortened sublimation (Schneid and Gieseler, 2008). However, these assumptions must be studied using higher volumes and concentrations to be accurate.

4.2.6.3 The effects of adding EC to SA

4.2.6.3.1 The effects of EC on the structure of the product

The main reason for using EC is to harden and toughen the composition with which EC is compatible. This property is related to its long chain β anhydroglucose units and the hydroxyl group in the EC structure (OH), as shown in Figure 31 (Murtaza, 2012). Based on the procedure discussed in section 3.2.14 and the results in section 4.1.7.1, Figure 24 shows that SA/EC hardened shapes when compared to SA. However, the final shape appeared as a collapsed product. It should be mentioned that, to obtain the required appearance when using EC, the low Mwt of EC must be added for two reasons. First, the components of this system (SA) are highly insoluble and require a low Mwt concentration to be used. Second, the stiffness and tensile strength of the product decreases when the concentration of EC is increased, which occurred when using the E class of this polymer (see section 1.3); therefore, an EC class N with a low Mwt are the appropriate choice in these conditions (Giri *et al.*, 2012; Mahnaj *et al.*, 2013; Murtaza, 2012).

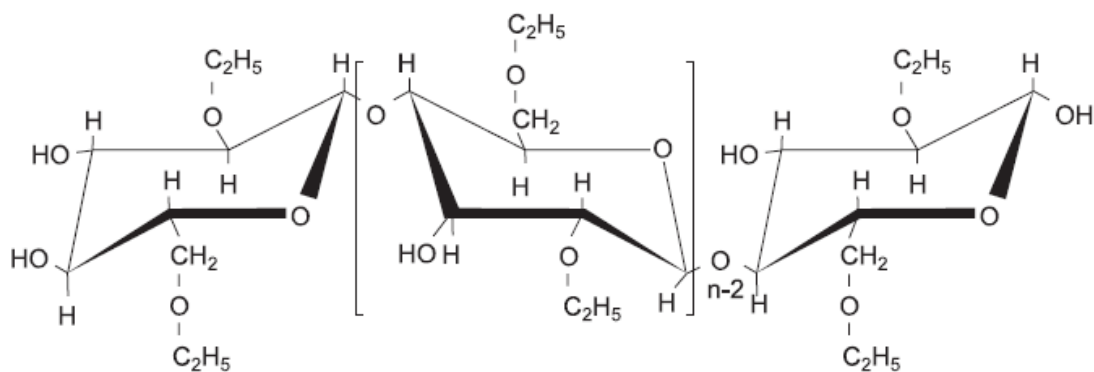


Figure 31: The chemical structure of EC polymer (adapted from Murtaza, 2012).

4.2.6.3.2 The effects of adding EC on SA primary drying times using the product thermocouple temperature.

Based on the procedure outlined in section 3.2.14 and the results presented in section 4.1.7, Figure 25 shows that 2.5 ml of EC/SA 5% reaches the end point of the primary drying time faster than pure SA, according to sample monitoring using a thermocouple sensor. Additionally, a two-way ANOVA analysis revealed statistically significant differences between the end point of primary drying for EC/SA 5% and for pure SA. It is possible that the EC provided similar behaviour as SA/PVA during the freeze-drying process, as discussed in detail in section 4.2.6.2.

As seen during all cycles of production, SA alone or within any prepared formulation and when the sublimation phase begins, largely decreases the temperature of the products because of the exothermic behaviour of the TEB (as discussed in section 4.2.4). However, this reaction did not occur with SA/EC 5%, as shown in Figure 25. The curve line of this product was nearly at the shelf temperature level and never dropped to less than -10 °C. There is no specific explanation for this dissimilarity because the data is limited to those obtained from SA/EC using TEB as a reaction solvent, but an explanation may be obtainable for two reasons:

- First, it is assumed that this exothermic behaviour may occur only with hydrophilic substances, e.g., AG, MAT and PVA; however, this is only true to a small extent because the reaction, i.e., a drastic drop in product temperature, also occurs with pure SA, which is extensively hydrophobic (see Figure 13).
- Second, it may correspond to the EC polymer properties as follows: Mahnaj *et al.* (2013) suggested that EC has a small crystalline phase with mostly amorphous regions, which is shown by XRD (see Appendix 6.6 XDR pattern of EC polymer). Davidovich-Pinhas *et al.* (2014) studied the properties of EC in detail using different Mwt and confirmed the suggestion made by Mahnaj *et al.* (2013). They also pointed out that by using DSC and SEM (Appendix 6.7), EC has a semi-crystalline structure with an amorphous background. This means that EC polymers have both a melting transition, which occurs in crystalline polymers, and a glass transition at temperatures ranging from 165–174 °C and 120–135 °C, respectively. These transitions are increased when the Mwt of the EC polymer is increased. Therefore, because of the assumption that the behaviour of TEB is exothermic, which is discussed in section 4.2.4, EC is expected to absorb high exothermic energy from other media to obtain the melting transition, i.e., an endothermic reaction, and avoid dropping the product temperature to -40 °C, as in other experiments. Consequently, the approximate collapse shape of SA/EC 5% (Figure 24) is formed because of the melting transition after EC absorbs heat as energy from other media. However, additional studies are required to confirm this assumption.

To summarise, according to the results and discussions of this section, all formulations, when added to SA, can produce stronger shapes than pure SA alone is able to, although most of the formulations were unexpectedly brittle or collapsed the shape. However, Table 3 includes different formulations and each formulations D and H after drying. It is clear from Table 3 that SA/PVA 5% provides the most acceptable shape (cake) and thickness (H). All

formulations could statistically decrease the end point of the primary drying time, when compared with the end point of SA, with the exception of MAT (according the two-way ANOVA analysis).

Table 3: The H and D of different formulations when adding different substances to 2.5 ml of SA during synthesis (according to 4.1 Results section).

Formulation	%	H (mm)	D (mm)
SA/AG	0.25	3.5	18
SA/AG	1	4.5	20
SA/MAT	1	3	20
SA/MAT	5	4	23
SA/PVA	5	5.3	26
SA/EC	5	4.4	22

Nevertheless, additional studies are required to determine the exact reasons for the different measurements obtained during the primary drying cycle because each formula exhibited different behaviour when combined with the TEB. Further experiments involving higher volumes, concentrations and cycles are required to determine which products can produce the sublimation stage quicker than pure SA can produce it.

4.2.7 The effects of recycled TEB

When preparing vials of SA for the mechanical drying phase, the remaining solvent inside the vials is called recycled TEB (in this study, this is the remaining solvent from the aging step). This solvent was collected and a hypothesis proposed that TEB can be reused to age other samples of SA without affecting the primary drying end point. According to the procedure discussed in section 3.2.16 and the results presented in section 4.1.8, Figure

26 shows that there are no statistically significant differences (analysed using two-way ANOVA) between the primary drying times when using pure TEB and recycled TEB to age 2.5 ml of SA. This is another benefit of using TEB as a solvent: it can be recycled to age another sample. Therefore, this result reduces the cost of the solvent because the aging step requires extensive amounts of TEB during the aging process (see section).

4.2.8 Separation of the liquid collected from the condenser

Although the procedure presented in section 3.2.17 for recycling the TEB during lyophilisation is very preliminary, the results in section 4.1.9 show that during day five of monitoring, the volumes of liquid collected from the condenser did not alter the remaining volumes of liquid in the cylinders (Figure 27). This means that all of the TEB evaporated at room temperature, and the remaining liquid consisted of water and impurities. This is a simple method for obtaining more TEB for further experiments and can be repeated by using the distillation apparatus to separate the TEB from other solvents using exact volumes.

5. Conclusions

5.1 Conclusion

Section 4.1 presents the results of using the TEB as a reaction solvent to prepare SA in freeze-drying process, and of preparing some successful formulations when combining SA with different substances. In addition, different sensors could show the end points of primary drying of SAs (pure or combined). This is considered a key element of detecting the sublimation time to minimise the cost of the lyophilisation cycle, since the primary drying phase is the longest step of this process. These results support hypothesis 3.2.1 (according to the methods in section 3.2.2 and the results in section 4.1.1) since the SAs were synthesised using TEB as a novel solvent in the freeze-drying cycle. Also, hypothesis 3.2.5 (according to the methods in section 3.2.6 and the results in section 4.1.3) was supported, because the largest volume required a long time to be sublimed compared to the smaller volumes.

Moreover, hypotheses 3.2.7 (methods section 3.2.8 and results section 4.1.4), 3.2.11.1 (methods section 3.2.12 and results section 4.1.5), 3.2.11.2 (methods section 3.2.13 and results section 4.1.6), and 3.2.11.3 (methods section 3.2.14 and results section 4.1.7) were all supported, since they could produce new formulations (SA/AG, SA/MAT, SA/PVA, and SA/EC, respectively) with unique properties and primary drying rates. However, not all the hypotheses were supported by the results. Hypothesis 3.2.3 (methods section 3.2.4 and results section 4.1.2) was rejected because using an acid or base alone could not gel the solution in the first step of SA production.

On the other hand, all hypotheses that used the thermocouple sensor, the Corillonite sensor, and the microbalance were supported by the results. Hypothesis 3.2.5 (methods section 3.2.6 and results section 4.1.3) was accepted since the thermocouple sensor could monitor the primary drying of SA by monitoring the temperature. Consequently, both parts of hypothesis 3.2.9 were supported by the results. First, the Corillonite sensor (methods section 3.2.10.1 and results section 4.1.4.5) determined the end point of the sublimation of SA using a signal analogue. Secondly, the microbalance

(methods section 3.2.10.2 and results section 4.1.4.6) measured the end point of the primary drying by using the weight loss of the product.

Furthermore, hypothesis 3.2.15.1 (methods section 3.2.16 and results section 4.1.8) was successfully supported, since using recycled TEB to age new SA samples showed no significant difference in primary drying rate compared to using pure TEB to age new SA samples. Also, hypothesis 3.2.15.2 (methods section 3.2.17) was consistent with the results that were illustrated in section 4.1.9, since the liquid collected from the condenser was separated when the TEB evaporated and remained impurities in the water.

5.2. Future work

The following investigations could continue the work done in this research:

1. Use a special freeze-drying cycle for each formulation (SA/AG, SA/MAT, SA/PVA, and SA/EC) to obtain the desired appearance, and to overcome the melting and collapsing problems, especially for SA/MAT.
2. Attempt to combine a higher molar ratio (higher concentration) of the above formulations with the SA product.
3. Use a distillation apparatus to separate the compositions of liquids collected from the condenser, then study the efficiency of the TEB.

6. Appendix:

6.1 The specific properties of Oct Temp/ thermocouple sensor

Temperature Range	-20 °C to +60 °C (-4 °F to +140 °F)		
Temperature Resolution	0.05 °C (0.09 °F)		
Calibrated Accuracy	±0.5 °C (0 °C to +50 °C)		
Remote Channel Thermocouple Types	J, K, T, E, R, S, B, N		
Thermocouple Connection	Female subminiature (SMP)		
Cold Junction Compensation	Automatic. based on internal channel		
Thermocouple	Range (°C)	Resolution	Accuracy
J	-210 to +760	0.1 °C	±0.5 °C
K	-270 to +1370	0.1 °C	±0.5 °C
T	-270 to +400	0.1 °C	±0.5 °C
E	-270 to +980	0.1 °C	±0.5 °C
R	-50 to +1760	0.5 °C	±2.0 °C
S	-50 to +1760	0.5 °C	±2.0 °C
B	+50 to +1820	0.5 °C	±2.0 °C
N	-270 to +1300	0.1 °C	±0.5 °C
Start Modes	Software programmable immediate start or delay start up to six months in advance.		
Real Time Recording	May be used with PC to monitor and record data in real time.		
Memory	500,000 readings per channel, channels can be disabled to increase memory.		
Reading Rate	4 readings per second up to 1 every 24 hours		
Calibration	Digital calibration through software		
Calibration Date	Automatically recorded within device		
Battery Type	9 Volt lithium or alkaline battery included, user replaceable		
Battery Life	18 months typical		
Data Format	Date and time stamped °C, °F, K, °R, mV, V		
Time Accuracy	±1 minute/month		
Computer Interface	USB (Interface cable required); 115,200 baud		
Software	XP SP3/Vista/Windows 7/Windows 8 (MadgeTech 4 only)		
Operating Environment	-20 °C to +60 °C (-4 °F to +140 °F), 0 %RH to 95 %RH non-condensing		
Dimensions	7.24 in x 2.7 in x 1.26 in (183 mm x 68 mm x 32 mm)		
Material	Black anodized aluminum		
Weight	17.3 oz (490 g)		
Approvals	CE		
Maximum Thermocouple Resistance	1000Ω <100Ω recommended		

6.2 Properties of Corillonite sensor

Microcontroller	ATmega328
Operating Voltage	5V
Input Voltage (recommended)	7-12V
Input Voltage (limits)	6-20V
Digital I/O Pins	14 (of which 6 provide PWM output)
Analogue Input pins	6
DC Current per I/O Pin	40 mA
DC Current for 3.3V Pin	50 mA
Flash Memory	32 KB (ATmega328) of which 0.5 KB used by bootloader
SRAM	2 KB (ATmega328)
EEPROM	1 KB (ATmega328)
Clock Speed	16 MHz
Led	1.7 volt small circus of light

6.3. Calculation of the molar ratio of MAT

6.3.1 MAT 1%: (Shawkat et al., 2012).

$$\text{MAT} = \frac{wt}{Mwt} \Rightarrow = \frac{0.2g}{182g/mole} = 1 \times 10^{-3} \text{ mole, Referred to as 1\% in the project}$$

6.3.2 MAT 5%

$$\text{MAT} = \frac{wt}{Mwt} \Rightarrow = \frac{1g}{182g/mole} = 5 \times 10^{-3} \text{ mole, Referred to as 5\% in the project}$$

6.4. Calculation the molar ratio of PVA

Mwt of PVA has different ranges and according to its hydrolysis

And therefore 12,000 was used

$$\text{PVA} = \frac{wt}{Mwt} \Rightarrow \frac{0.2g}{12000g/mole} = 16 \times 10^{-6} \text{ mole, Referred to as 5\% in the project}$$

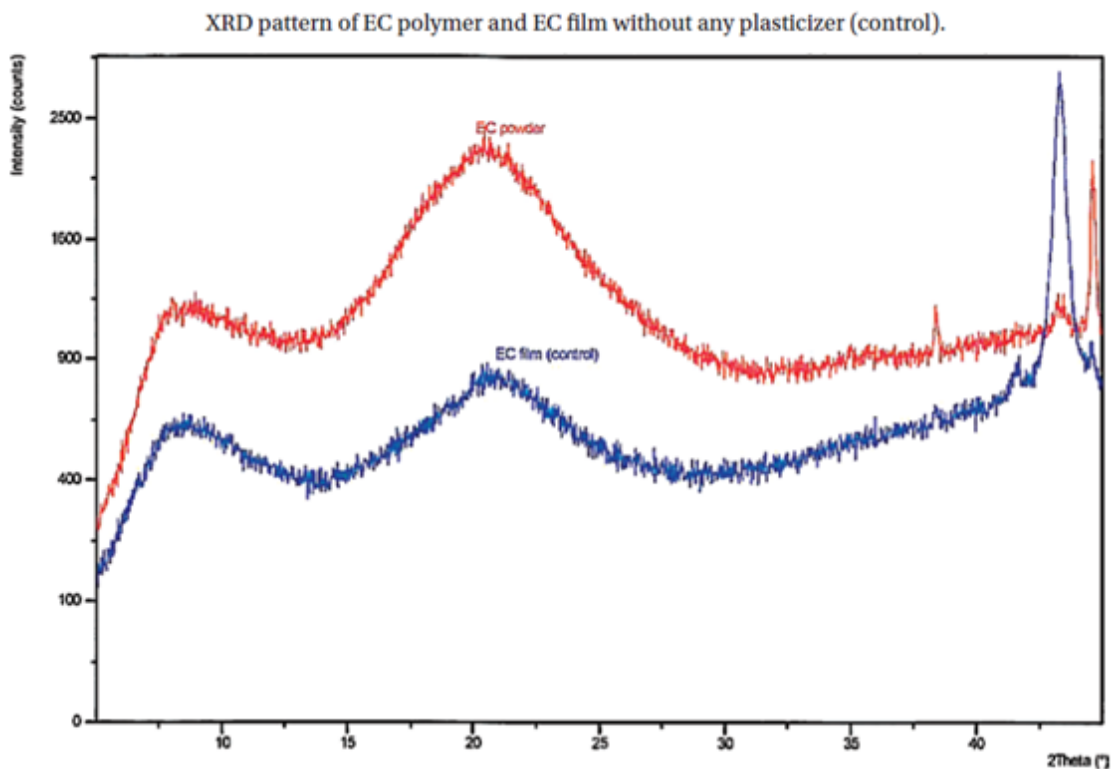
6.5 Calculation the molar ratio of EC

Mwt of EC 246.3001 g/mole

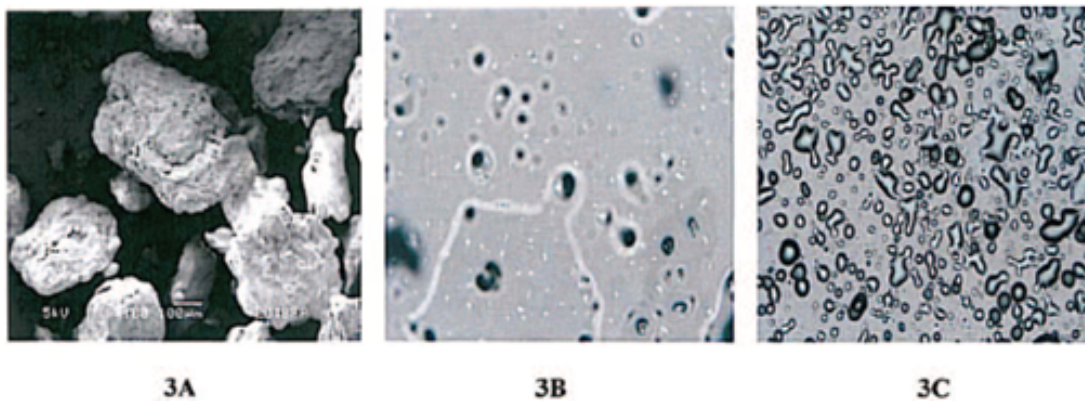
$$\text{EC} = \frac{wt}{Mwt} \Rightarrow \frac{1.3g}{246.3001g/mole} = 5 \times 10^{-3} \text{ mole, Referred to as 5\% in the project}$$

project

6.6. XDR pattern of EC polymer



6.7 EC polymer under SEM



EC polymer under SEM (A), under polarized light microscope (B) and under hot-stage microscope at about 180°C (C).

References

- Adams, G. (2007). 'The Principles of Freeze-Drying', In Day, J. G. and Stacey, G. (ed.). *Cryopreservation and freeze-drying protocols* (Vol. 368). Springer Science and Business Media. p. 15-38.
- Akers, M. J. (2013). 'Parenteral Preparation' In Felton, L. A. (ed.). *Remington Essentials of Pharmaceutics*. London: Pharmaceutical Press, p. 495-535.
- Badamasi, Y. A. 2014. "The working principle of an Arduino." In *Electronics, Computer and Computation (ICECCO), Abuja, Nigeria.IEEE*.
- Bandyopadhyay, A., De Sarkar, M. and Bhowmick, A. K. (2005). Poly (vinyl alcohol)/silica hybrid nanocomposites by sol-gel technique: Synthesis and properties. *Journal of materials science*, **40**(19), 5233-5241.
- Bellissent-Funel and Teixeira (2010). 'Structural and Dynamic Properties of Bulk and Confined Water', In Rey, L. and May, J. (ed.). *Freeze-Drying/Lyophilization Of Pharmaceutical And Biological Products*, New York: Marcel Dekker. p. 29-51.
- Bisson, A., Rigacci, A., Lecomte, D., Rodier, E. and Achard, P. (2003). Drying of silica gels to obtain aerogels: phenomenology and basic techniques. *Drying technology*, **21**(4), 593-628.
- Bosca, S., Corbellini, S., Antonello A. Barresi, A. A. and Fissore, D. (2013). Freeze-Drying Monitoring Using a New Process Analytical Technology: Toward a "Zero Defect" Process. *Drying Technology: An International Journal* [Online], **31**, 1744-1755. Available from: <http://dx.doi.org/10.1080/07373937.2013.807431> [Accessed 20 August 2015].
- Brinker, C. J. and Scherer, G. W. (2013). *Sol-gel science: the physics and chemistry of sol-gel processing*. Academic press.
- Bronzino, J. D. and Peterson, D. R. (2014). *Biomedical engineering fundamentals*. CRC Press, [Online]. Available from: <https://books.google.co.uk/books?hl=en&lr=&id=N4iZBQAAQBAJ&oi=fnd&pg=PP1&dq=Bronzino,+J.D.,+and+D.R.+Peterson.+2014.+Biomedical+Engineering+Fundamentals+%28Taylor+%26+Francis%29.&ots=t6r-CKclTL&sig=xB0Px1alBYrczbF6O1GY4bfk-QY#v=onepage&q&f=false> [Accessed 1 August 2015].
- Bronzino, J. D. and Peterson, D. R. (2014). *Biomedical engineering fundamentals*. CRC Press.
- Brydson, J.A. (2013). *Plastics Materials*, Elsevier Science, [Online]. Available from:

https://books.google.co.uk/books?id=wmohBQAAQBAJ&printsec=frontcover&source=gbg_summary_r&cad=0#v=onepage&q&f=false [Accessed 26 August 2015].

Creighton, T. E. (2010). *The physical and chemical basis of molecular biology*. Helvetian Press.

Daintith, J. and Martin, E. (2010), *A Dictionary Of Science*. Oxford ; New York : Oxford University Press, [Online]. Available from: <https://app.knovel.com/web/toc.v/cid:kpDSE00001> [Accessed 20 July 2015].

Davidovich-Pinhas, M., Barbut, S. and Marangoni, A. G. (2014). Physical structure and thermal behavior of ethylcellulose. *Cellulose*, **21**(5), 3243-3255.

DeMerlis, C. C. and Schoneker, D. R. (2003). Review of the oral toxicity of polyvinyl alcohol (PVA). *Food and Chemical Toxicology* [Online], **41**(3), 319-326. Available from: https://scholar.google.co.uk/scholar?q=Review+of+the+oral+toxicity+of+polyvinyl+alcohol+%28PVA%29&btnG=&hl=en&as_sdt=0%2C5 [Accessed 28 August 2015].

Dietrich, C., Maurer, M., Roehl, H. and Frieß, W. (2010). 'Pharmaceutical Packaging for Lyophilization Applications', In Rey, L. and May, J. (ed.). *Freeze-Drying/Lyophilization Of Pharmaceutical And Biological Products*, New York: Marcel Dekker. p. 383-395.

Djabourov, M., Nishinari, K. and Ross-Murphy, S. B. (2013). *Physical gels from biological and synthetic polymers*. Cambridge University Press.

Duff, M. and Towey, J. (2010). Two Ways to Measure Temperature using thermocouples feature simplicity, accuracy, and flexibility. 44-10, [Online]. Available from: <http://www.analog.com/library/analogDialogue/archives/44-10/thermocouple.html/thermocouple.pdf> [Accessed 2 August 2015].

Egeberg, E. D. and Engell, J. (1989). Freeze drying of silica gels prepared from siliciumethoxid. *Le Journal de Physique Colloques* [Online], **50**(C4), C4-23. Available from: https://scholar.google.co.uk/scholar?q=Freeze+drying+of+silica+gels+prepared+from+siliciumethoxid&btnG=&hl=en&as_sdt=0%2C5 [Accessed 2 August 2015].

Estella, J., Echeverría, J. C., Laguna, M. and Garrido, J. J. (2007). Effects of aging and drying conditions on the structural and textural properties of silica gels. *Microporous and mesoporous materials*, **102**(1), 274-282.

- Fissore, D. (2013). 'Freeze drying of pharmaceuticals', in Swarbrick, J. (ed.). *Encyclopedia Of Pharmaceutical Science And Technology*. Boca Raton: CRC Press, Taylor and Francis Group, p. 1723-1734.
- Franks, F. and Auffret, T. (2007). *Freeze-Drying Of Pharmaceuticals And Biopharmaceuticals*. Cambridge.
- Giri, T. K., Kumar, K., Alexander, A., Badwaik, H. and Tripathi, D. K. (2012). A novel and alternative approach to controlled release drug delivery system based on solid dispersion technique. *Bulletin of Faculty of Pharmacy, Cairo University* [Online], **50**(2), 147-159. Available from: https://scholar.google.co.uk/scholar?q=A+novel+and+alternative+approach+to+controlled+release+drug+delivery+system+based+on+solid+dispersion+technique&btnG=&hl=en&as_sdt=0%2C5 [Accessed 20 July 2015].
- Gould, G., Ou, D., Begag, R. and Rhine, W. E. (2008). Highly-transparent polymer modified silica aerogels. *Polymer Preprints*, **49**(2), 534.
- Haereid, S., Dahle, M., Lima, S. and Einarsrud, M. A. (1995). Preparation and properties of monolithic silica xerogels from TEOS-based alcogels aged in silane solutions. *Journal of non-crystalline solids*, **186**, 96-103.
- Hassan, C. M. and Peppas, N. A. (2000). Structure and applications of poly (vinyl alcohol) hydrogels produced by conventional crosslinking or by freezing/thawing methods. In *Biopolymers: PVA Hydrogels, Anionic Polymerisation Nanocomposites*, 37-65. Springer Berlin Heidelberg, [Online]. Available from: https://scholar.google.co.uk/scholar?q=structure+and+applications+of+poly+vinyl+alcohol+hydrogels+produced+by+conventional+crosslinking+or+by+freezing%2Fthawing+methods&btnG=&hl=en&as_sdt=0%2C5 [Accessed 30 August 2015].
- Hung, P. C., Irwin, G., Kee, R. and McLoone, S. (2005). Difference equation approach to two-thermocouple sensor characterization in constant velocity flow environments. *Review of Scientific Instruments* [Online], **76**(2), 024902. Available from: https://scholar.google.co.uk/scholar?q=%27Difference+equation+approach+to+twothermocouple+sensor+characterization+in+constant+velocity+flow+environments&btnG=&hl=en&as_sdt=0%2C5 [Accessed 22 August 2015].
- Kerlin, T. W. and Johnson, M. (1999). *Practical Thermocouple Thermometry*. Instrument Society of America.
- Khairnar, S. , Kini, R., Harwalkar, M., Salunkhe, K. and Chaudhari, S.R. (2013). A Review on Freeze Drying Process of Pharmaceuticals. *International Journal of Research in Pharmacy and Science* [Online], **4**(1), 76-94. Available from: www.ijrpsonline.com [Accessed 3 August 2015].
- Kim, A. I., Akers, M. J. and Nail, S. L. (1998). The physical state of mannitol after freeze-drying: Effects of mannitol concentration, freezing rate, and a

noncrystallizing cosolute. *Journal of pharmaceutical sciences* [Online], **87**(8), 931-935. Available from:

<https://scholar.google.co.uk/scholar?q=The+Physical+State+of+Mannitol+after+Freeze->

[Drying%3A+Effects+of+Mannitol+Concentration%2C+Freezing+Rate%2C+and+a+Noncrystallizing+Cosolute&btnG=&hl=en&as_sdt=0%2C5](https://scholar.google.co.uk/scholar?q=The+Physical+State+of+Mannitol+after+Freeze-Drying%3A+Effects+of+Mannitol+Concentration%2C+Freezing+Rate%2C+and+a+Noncrystallizing+Cosolute&btnG=&hl=en&as_sdt=0%2C5) [Accessed 4 August 2015].

Kim, C. E., Yoon, J. S. and Hwang, H. J. (2008). Synthesis of nanoporous silica aerogel by ambient pressure drying. *Sol-Gel Science and Technology* [Online], **52**, 49-52. Available from:

<http://link.springer.com/article/10.1007%2Fs10971-008-1828-7> [Accessed 14 August 2015].

Mahnaj, T., Ahmed, S. U. and Plakogiannis, F. M. (2013). Characterization of ethyl cellulose polymer. *Pharmaceutical development and technology* [Online], **18**(5), 982-989. Available from:

https://scholar.google.co.uk/scholar?q=Characterization+of+ethyl+cellulose+polymer&btnG=&hl=en&as_sdt=0%2C5 [Accessed 20 August 2015].

Maleki, H., Durães, L. and Portugal, A. (2013). An overview on silica aerogels synthesis and different mechanical Reinforcing strategies. *Journal of Non-Crystalline Solids* [Online], **385**, 55-74. Available from:

<http://www.sciencedirect.com/science/article/pii/S002230931300522X> [Accessed 3 August 2015].

Mehta, M., Bhardwaj, S. P. and Suryanarayanan, R. (2013). Controlling the physical form of mannitol in freeze-dried systems. *European Journal of Pharmaceutics and Biopharmaceutics* [Online], **85**(2), 207-213. Available from: https://scholar.google.co.uk/scholar?q=Controlling+the+physical+form+of+mannitol+in+freeze-dried+systems&btnG=&hl=en&as_sdt=0%2C5 [Accessed 9 August 2015].

Mellor, J.D. (1978). *Fundamentals of Freeze-Drying*: London: Academic Press.

Mizuno, T., Nagata, H. and Manabe, S. (1988). Attempts to avoid cracks during drying. *Journal of Non-Crystalline Solids*, **100**(1), 236-240.

Murtaza, G. (2012). Ethylcellulose microparticles: a review. *Acta Pol Pharm* [Online], **69**(1), 11-22. Available from:

https://scholar.google.co.uk/scholar?q=Ethylcellulose+microparticles%3A+a+review%27%2C+Acta+Pol+Pharm&btnG=&hl=en&as_sdt=0%2C5

[Accessed 20 July 2015].

Novak, B. M., Auerbach, D. and Verrier, C. (1994). Low-density, mutually interpenetrating organic-inorganic composite materials via supercritical drying techniques. *Chemistry of materials*, **6**(3), 282-286.

- Passot, S., Tre´le´a, I. C., Marin, M. and Fonseca, F. (2010). ‘The Relevance of Thermal Properties for Improving Formulation and Cycle Development: Application to Freeze-Drying of Proteins’, In Rey, L. and May, J. (ed.). *Freeze-Drying/Lyophilization Of Pharmaceutical And Biological Products*, New York: Marcel Dekker. p. 136-166.
- Patel, S. M. and Pikal, M. (2009). Process Analytical Technologies (PAT) in freeze-drying of parenteral products. *Pharmaceutical Development and Technology* [Online], **14**(6),567–587. Available from: <http://www.ncbi.nlm.nih.gov/pubmed/19883247> [Accessed 10 July 2015].
- Patel, S. M., Doen, T. and Pikal, M. J. (2010). Determination of End Point of Primary Drying in Freeze-Drying Process Control. *American Association of Pharmaceutical Scientists* [Online], **11**(1) 73-84. Available from: <http://www.ncbi.nlm.nih.gov/pmc/articles/PMC2850457/> [Accessed 22 July 2015].
- Pons, A., Casas, L., Estop, E., Molins, E., Harris, K. D. M. and Xu, M. (2012). A new route to aerogels: Monolithic silica cryogels. *Journal of Non-Crystalline Solids* [Online], **358**(3), 461-469. Available from: https://scholar.google.co.uk/scholar?q=a+new+route+to+aerogels+%3A+monolithic+silica+cryogels&btnG=&hl=en&as_sdt=0%2C5 [Accessed 16 August 2015].
- Rey, L. (2010). ‘Glimpses into the Realm of Freeze-Drying: Classical Issues and New Ventures’, In Rey, L. and May, J. (ed.). *Freeze-Drying/Lyophilization Of Pharmaceutical And Biological Products*, New York: Marcel Dekker. p. 1-28.
- Roth, C., Winter, G. and Lee, G. (2001). Continuous measurement of drying rate of crystalline and amorphous systems during freeze-drying using an in situ microbalance technique. *Journal of pharmaceutical sciences* [Online], **90**(9), 1345-1355. Available from: https://scholar.google.co.uk/scholar?q=Continuous+measurement+of+drying+rate+of+crystalline+and+amorphous+systems+during+freeze%E2%80%90drying+using+an+in+situ+microbalance+technique&btnG=&hl=en&as_sdt=0%2C5 [Accessed 13 August 2015].
- Schneid, S. and Gieseler, H. (2008). Effect of concentration, vial size and fill depth on product resistance of sucrose solutions during freeze drying, [Online]. Available from: https://scholar.google.co.uk/scholar?q=Effect+of+concentration%2C+vial+size+and+fill+depth+on+product+resistance+of+sucrose+solutions+during+freeze+drying.&btnG=&hl=en&as_sdt=0%2C5 [Accessed 13 July 2015].
- Schneid, S. C., Gieseler, H., Kessler, W. J., Luthra, S. A. and Pikal, M. J. (2011). Optimization of the Secondary Drying Step in Freeze Drying Using TDLAS Technology. *Pharmaceutical Science Technology* [Online], **12**(1) 379-387. Available from: <http://www.ncbi.nlm.nih.gov/pubmed/21359604> [Accessed 1 August 2015].

- Searles, J. A. (2010). 'Freezing and Annealing Phenomena in Lyophilization', In Rey, L. and May, J. (ed.). *Freeze-Drying/Lyophilization Of Pharmaceutical And Biological Products*, New York: Marcel Dekker. p. 52-81.
- Shawkat, H., Westwood, M. M. and Mortimer, A. (2012). Mannitol: a review of its clinical uses. *Continuing Education in Anaesthesia, Critical Care and Pain* [Online], **12**(2), 82-85. Available from: https://scholar.google.co.uk/scholar?q=Mannitol%3A+a+review+of+its+clinical+uses&btnG=&hl=en&as_sdt=0%2C5 [Accessed 4 July 2015].
- Sinko, P., Singh, Y. and Martin, A. (2011). *Martin's Physical Pharmacy And Pharmaceutical Sciences: Physical Chemical And Biopharmaceutical Principles In The Pharmaceutical Sciences*, Baltimore, MD: Lippincott Williams and Wilkins.
- Smirnova, I. and Arlt, W. (2004). Synthesis of silica aerogels and their application as drug delivery system. *Supercritical fluids as solvents and reaction media*, 381, [Online]. Available from: https://scholar.google.co.uk/scholar?q=Synthesis+of+silica+aerogels+and+their+application+as+drug+delivery+system&btnG=&hl=en&as_sdt=0%2C5 [Accessed 14 July 2015].
- Strøm, R. A., Masmoudi, Y., Rigacci, A., Petermann, G., Gullberg, L., Chevalier, B. and Einarsrud, M. A. (2007). Strengthening and aging of wet silica gels for up-scaling of aerogel preparation. *Journal of sol-gel science and technology*, **41**(3), 291-298.
- Su, L. F., Miao, L., Tanemura, S. and Xu, G. (2012). Low-cost and fast synthesis of nanoporous silica cryogels for thermal insulation applications. *Science and Technology of Advanced Materials* [Online], **13**(3), 1-6. Available from: https://scholar.google.co.uk/scholar?hl=en&as_sdt=0,5&q=low-cost+and+fast+synthesis+of+nanoporous+silica+cryogels+for+thermal+insulation+application [Accessed 12 August 2015].
- Sundararajan, P. R. and Islam, M. R. (2009). 'Poly(vinyl alcohol)' In Mark, J. E. (ed.). *Polymer Data Handbook (2nd Edition)*. Oxford University Press. p. 1116-1129, [Online]. Available from: <http://app.knovel.com/hotlink/toc/id:kpPDHE0004/polymer-data-handbook/polymer-data-handbook> [Accessed 20 August 2015].
- Tamaki, R. and Chujo, Y. (1998). Synthesis of poly (vinyl alcohol)/silica gel polymer hybrids by in-situ hydrolysis method, [Online]. Available from: https://scholar.google.co.uk/scholar?q=Synthesis+of+poly+%28vinyl+alcohol%29%2Fsilica+gel+polymer+hybrids+by+insitu+hydrolysis+method%27.&btnG=&hl=en&as_sdt=0%2C5 [Accessed 20 July 2015].
- Tan, C. S., Ingeen C. W. V. and Staplers, J. A. (2007). 'Freeze-Drying Fungi Using a Shelf-Freeze Drier; In Day, J. G., and Stacey, G. (ed.). *Cryopreservation and*

freeze-drying protocols (Vol. **368**). Springer Science and Business Media. p. 119-126.

Wang, X. D., Wolfbeis, O. S. and Meier, R. J. (2013). Luminescent probes and sensors for temperature. *Chemical Society Reviews* [Online], **42**(19), 7834-7869. Available from:

https://scholar.google.co.uk/scholar?q=Luminescent+probes+and+sensors+for+temperature&btnG=&hl=en&as_sdt=0%2C5 [Accessed 2 July 2015].

Ward, K. R. and Matejtschuk, P. (2010). 'The Use of Microscopy, Thermal Analysis, and Impedance Measurements to Establish Critical Formulation Parameters for Freeze-Drying Cycle Development', In Rey, L. and May, J. (ed.). *Freeze-Drying/Lyophilization Of Pharmaceutical And Biological Products*, New York: Marcel Dekker. p. 112-135.

Yang, Y. (2009). 'Ethylcellulose' In Mark, J. E. (ed.). *Polymer Data Handbook (2nd Edition)*. Oxford University Press. p. 146-151, [Online]. Available from: http://app.knovel.com/web/view/swf/show.v/rcid:kpPDHE0004/cid:kt006PVKY5/viewerType:pdf/root_slug:polymerdatahandbook?cid=kt006PVKY5&page=5&bq=Poly%28viny1%20alcohol%29%20P.%20R.%20Sundararajan%20and%20Molla%20Rafique1%20Islam&b-subscription=TRUE&bgroupby=true&b-search-type=tech-reference&b-sorton=default&btocid=kpPDHE0004&b-toc-root-slug=polymer-data-handbook&b-toc-url-slug=ethylcellulose&b-toctitle=Polymer%20Data%20Handbook%20%282nd%20Edition%29 [Accessed 11 August 2015].